

Unraveling the Mott-Peierls intrigue in Vanadium dioxide

F. Grandi,^{1,2} A. Amaricci,^{1,3} and M. Fabrizio¹

¹*Scuola Internazionale Superiore di Studi Avanzati (SISSA), Via Bonomea 265, I-34136 Trieste, Italy*

²*Department of Physics, University of Erlangen-Nürnberg, 91058 Erlangen, Germany*

³*CNR-IOM DEMOCRITOS, Istituto Officina dei Materiali,*

Consiglio Nazionale delle Ricerche, Via Bonomea 265, I-34136 Trieste, Italy

(Dated: March 13, 2020)

Vanadium dioxide is one of the most studied strongly correlated materials. Nonetheless, the intertwining between electronic correlation and lattice effects has precluded a comprehensive description of the rutile metal to monoclinic insulator transition, in turn triggering a longstanding “the chicken or the egg” debate about which comes first, the Mott localisation or the Peierls distortion. Here, we suggest that this problem is in fact ill-posed: the electronic correlations and the lattice vibrations conspire to stabilise the monoclinic insulator, and so they must be both considered not to miss relevant pieces of the VO₂ physics. Specifically, we design a minimal model for VO₂ that includes all the important physical ingredients: the electronic correlations, the multi-orbital character, and the two components antiferrodistortive mode that condenses in the monoclinic insulator. We solve this model by dynamical mean-field theory within the adiabatic Born-Oppenheimer approximation. Consistently with the first-order character of the metal-insulator transition, the Born-Oppenheimer potential has a rich landscape, with minima corresponding to the undistorted phase and to the four equivalent distorted ones, and which translates into an equally rich thermodynamics that we uncover by the Monte Carlo method. Remarkably, we find that a distorted metal phase intrudes between the low-temperature distorted insulator and high-temperature undistorted metal, which sheds new light on the debated experimental evidence of a monoclinic metallic phase.

I. INTRODUCTION

Vanadium dioxide (VO₂) is a transition metal compound with tremendous potential for technological applications, essentially in reason of its nearly room temperature metal-to-insulator transition [1–10]. Over the years, VO₂ has been subject to an intense investigation, which dates back to the first decades of the last century [11–20], but that is yet alive [21–23] and, to some extent, debated [24–30]. At the critical temperature $T_c \sim 340$ K and ambient pressure, VO₂ undergoes a first-order transition from a metal ($T > T_c$) to an insulator ($T < T_c$) [31, 32], both phases being paramagnetic [33–35]. In concomitance with the metal-insulator transition, a structural distortion occurs from a high-temperature rutile (R) structure to a low temperature monoclinic (M1) one.

The crystal structure of rutile VO₂ is formed by equally spaced apart Vanadium atoms sitting at the centre of edge-sharing oxygen octahedra that form linear chains along the R c -axis, which we shall denote as c_R , see Fig. 1. The tetragonal crystal field splits the $3d$ -manifold into two higher e_g and three lower t_{2g} levels. In the oxidation state V⁴⁺, the single valence electron of Vanadium can, therefore, occupy any of the three t_{2g} orbitals, which are in turn distinguished into a singlet a_{1g} (or $d_{||}$) and a doublet e_g^π (or d_{π^*}), having, respectively, bonding and non-bonding character along the c_R -axis. The M1 phase is instead characterised by an anti-ferroelectric displacement of each Vanadium away from the centre of the octahedra, see Fig. 1, so that the above-mentioned chains, from being straight in the R phase, turn zigzag and dimerise [36, 37].

A simple portrait of the transition in VO₂ was proposed in 1971 by Goodenough [38]. According to his proposal, the basal-plane component of the anti-ferroelectric distortion raises the energy of e_g^π with respect to the a_{1g} [39]. In addition, the c_R component of the distortion, which drives the chain dimerisation, opens a hybridisation gap between bonding and anti-bonding combinations of the a_{1g} . For large enough crystal field splitting and hybridisation gap, the bonding combination of the a_{1g} fills completely, while the anti-bonding as well as the e_g^π get empty, hence the insulating behaviour. The Goodenough’s mechanism for the metal-insulator transition in VO₂ thus relies on a single-particle description: the Peierls instability of the quasi-one-dimensional a_{1g} band that becomes half-filled after the growth of the crystal field drained the e_g^π orbital.

However, Pouget et al. [40] and later Zylbersztein and Mott [41] soon after argued that the role of electronic correlation cannot be neglected as in the Goodenough’s scenario. Indeed, a tiny $\sim 0.2\%$ substitution of V with Cr changes the low-temperature insulator from the M1 crystal structure to a new monoclinic phase, named M2, where dimerised and zigzag chains alternate [34, 42]. The M2 phase can be also stabilised under hydrostatic pressure or uniaxial stress [31, 32, 40, 43–45]. In addition, a triclinic (T) phase with intermediate structural properties [42] was shown to intrude between M1 and M2. The zigzag undimerised chains in M2 are still insulating and display magnetic properties akin those of a spin-1/2 anti-ferromagnetic Heisenberg chain [40, 42, 46]. This likeness can be rationalised only invoking sizeable electronic correlations. Given the low concentration of substitutional Chromium or the small value of uniaxial stress required

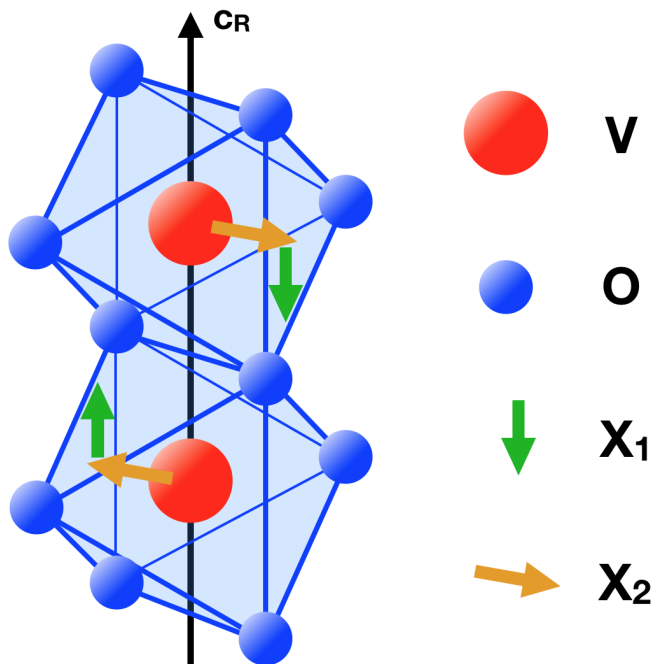


Figure 1. (Color online) The rutile crystal structure, where the large (small) spheres represent Vanadium (oxygen) atoms. A cartoon of the X_1 and X_2 lattice distortions is also depicted, where the X_1 component acts as a dimerisation along the c_R axis and the X_2 component acts as a tilting in the perpendicular plane. The monoclinic M1 phase is actually characterised by finite displacements both of X_1 and X_2 .

to stabilise M2, it is reasonable to conclude that M1 must be as correlated as M2 [47–50].

We believe that, even though electronic correlations are likely necessary, they are nonetheless not sufficient to explain the phase diagram of VO_2 . It is known that a strong enough repulsion may drive a Mott transition in a three-band Hubbard model at the density of one electron per site [51]. Therefore, it is well possible that the insulating phase of VO_2 is driven by correlations alone, and that the structural distortion below T_c is just the best way the Mott insulator can freeze the residual spin and orbital degrees of freedom to get rid of their entropy. However, should that be the case, VO_2 would most likely remain insulating even above T_c , which is not the case, all the more so because $k_B T_c$ is more than one order of magnitude smaller than the optical gap in the M1 phase [52]. For the same reason, we must exclude a transition merely driven by the larger electronic entropy of the metal.

We are thus inclined to believe that the structural distortion is also necessary to stabilise the insulating phase in VO_2 , but, once again, not sufficient in view of the behaviour of the M2 phase, and of the *bad metal* character of the R phase [53–55]. It is therefore quite likely that Goodenough’s scenario is after all correct, though it requires an active contribution from electronic correlations.

Indeed, different DFT-based calculations, which should properly account for the effects of the lattice dis-

ortion on the electronic structure, though within an independent-particle scheme, do not agree one with another, and none explains at once all experiments. For instance, straight LDA or GGA methods do not find any gap opening in M1 and M2 phases [56, 57]. Such gap is instead recovered by GW [58–60] or LDA+U [61–63], in all its variants. However, GW does not give easy access to the total energy, and therefore it does not explain why low temperatures should favour the M1 distorted phase against the rutile undistorted one. In turns, LDA+U or GGA+U calculations, known to overemphasise the exchange splitting, predict the existence of local moments even in the rutile phase [61–63], not observed in experiments [64]. Relatively recent calculations based on HSE hybrid functionals bring even worst results: both rutile and M1 phases are predicted to be magnetically ordered insulators, with the former lower in energy [65, 66], even though earlier calculations were claimed to be more in accordance with experiments [25]. In turn, mBJ exchange potentials seem to predict the proper conducting behaviour of the R and M1 phases, as well as their lack of magnetism [67], which is erroneously predicted to occur also in the M2 phase [63]. This suggests that suppression of magnetic moments is somehow the rule of mBJ functionals applied to VO_2 , which only by chance is the correct result for R and M1 phases. Finally, calculations based on PBE0 hybrid functionals properly account for the magnetic and electronic properties of M1 and M2 phases, but predict ferromagnetism in the rutile structure, at odds with experiments [33], as well as the existence of a never observed ferromagnetic and insulating monoclinic phase, dubbed M0 [68], also predicted by PBEsol functionals [69].

One might expect that combining *ab-initio* techniques with many-body tools, e.g., DFT with dynamical mean-field theory (DMFT) [70], should work better and finally provide uncontroversial results in accordance with experiments. Unfortunately, different calculations by state-of-the-art DFT+DMFT methods do not even agree about an unanimous view of the M1 monoclinic phase. Specifically, M1 has been regarded from time to time as a correlation-assisted Peierls insulator [24, 71], or, vice versa, as a Peierls-assisted Mott insulator [72], or, finally, as a genuine Mott insulator [26, 73, 74].

In view of the above controversial results, we think it is worth desisting from describing VO_2 straight from first principles, and rather focusing on a minimal model, which can include all the ingredients that are, by now, widely accepted to be essential. As we mentioned, electron-electron correlations must play an important role and thus need to be included and handled in a truly many-body scheme. At the meantime, the coupling of the electrons to the lattice is equally important and must be included as well. We earlier mentioned that the monoclinic distortion in the M1 phase actually entails two different antiferrodistortive components: the basal-plane displacement of V from the octahedron centre, resulting into a zigzag shape of the formerly straight chains, and

the out-of-plane displacement that produces the chain dimerisation. The two phenomena may actually occur separately, as indeed proposed by Goodenough [38], who argued that, generically, the basal-plane distortion should appear at higher temperatures than dimerisation. Indeed, time-resolved spectroscopy measurements during a photoinduced monoclinic-to-rutile transition have shown that dimerisation melts on earlier time-scales than the basal-plane displacement [37, 75, 76], which therefore must be distinct and actually more robust than the former. We must mention, however, that this conclusion does not agree with other experiments [77–80]. More convincing evidence is offered by the monoclinic metal that intrudes, under equilibrium conditions, between rutile metal and monoclinic insulator at ambient pressure [81–84], and nor just above a critical pressure as originally believed [85]. This phase might correspond to a crystal structure where dimerisation is almost melted unlike the zigzag distortion [69, 83], so that e_g^π are still above the a_{1g} , though the dimerisation is too weak to stabilise at that temperature an hybridisation gap within the a_{1g} band [27]. Even the disappearance prior to the metal-insulator transition [86] of the so-called singlet peak, which is associated to dimerisation and observed in optics, can be regarded as a consequence of the melting of dimerisation preceding the complete monoclinic-to-rutile transformation. All the above experimental facts point to the need to treat separately the basal-plane displacement and the out-of-plane one. Finally, the importance of the basal plane antiferrodistortive mode suggests the last ingredient to be considered: the multi-orbital physics. This aspect was originally emphasised by Goodenough [38] and successively confirmed by many optical measurements [52, 87, 88].

To summarise, we shall consider a microscopic model which includes the following relevant features:

1. the electron-electron correlations and the coupling to the lattice distortion [46, 53, 89–110];
2. the existence of two different antiferrodistortive components, each playing its own distinctive role [37, 38, 75];
3. the multi-orbital physics [38, 52, 87, 88].

with the minimal requirement of capturing, at least at a qualitative level, the following aspects of the VO_2 physics:

- A. the existence of an undistorted paramagnetic metal and a monoclinic distorted insulator [43, 111–114];
- B. the first-order character of the transition between them [18, 115–125];
- C. the possible existence of an intermediate monoclinic metal [81–83, 126–134];

Many models have been already put forth to describe VO_2 . However, most of them focus either on the role

of the electron-electron correlations, or on that of the electron-lattice coupling [27, 29, 135–148], and thus do not allow accessing in a single framework the whole VO_2 phase diagram, e.g., the points A., B. and C. above. Despite that, we must mention that the purely electronic Dimer Hubbard Model presented in [27], which by construction is not able to capture the monoclinic to rutile phase transition, is nevertheless able to describe some of the observed features of the monoclinic metal, like the MIR peak in the optical conductivity observed in [54]. There are actually some exceptions where electron-electron and electron-lattice interactions have been considered on equal footing [149–151]. In particular, the model studied in [150] includes explicitly all ingredients listed above. However, therein it is assumed a small bandwidth of the a_{1g} -derived band as compared to the e_g^π one, which contradicts LDA calculations [56]. Moreover, [150] includes the two distinct effects of the monoclinic distortion, but parametrized by a single displacement variable. In this way they preclude the possibility to describe the emergence of the monoclinic metal that seems to be observed experimentally. Furthermore, the mean-field treatment of the electron-electron interaction, despite its strength being comparable to the conduction bandwidth, yields not surprisingly to the formation of local moments in the rutile metal, not in accordance with magnetic measurements [64]. This negative result, highlighted by the same authors of Ref. [150], solicits for a more rigorous treatment of the interaction.

This is actually the scope of the present work, which is organised as follows. In Sec. II we introduce a simple model that includes the three ingredients previously outlined, which we believe should capture the main physics of Vanadium dioxide. In Sec. III we discuss the dynamical mean-field theory (DMFT) approach to the model Hamiltonian, and presents in Sec. III A its ground state phase diagram. In Sec. IV we discuss the insulator-metal transition that occurs in our model upon raising the temperature. In Sec. IV A we discuss the case in which such transition is driven solely by the electronic entropy, hence neglecting the lattice contribution to entropy, whereas in Sec. IV B the opposite case. We will show that the latter situation is rather suggestive, since it foresees different transition temperatures of the two antiferrodistortive components, as predicted by Goodenough [38]. In turn, this result might explain the evidence supporting the existence of a monoclinic metal phase. Finally, Sec. V is devoted to concluding remarks.

II. THE MODEL

As we mentioned, the orbitals that are relevant to describe the physics of VO_2 are the Vanadium $3d - t_{2g}$ ones, comprising the a_{1g} singlet and e_g^π doublet, which host a single conduction electron. We believe that in this circumstance the doublet nature of the e_g^π is not truly essential; what really matters is the distinction between

a_{1g} and e_g^π based on their bonding character with the ligands and response to atomic displacement. Therefore, in order to simplify our modelling without spoiling the important physics, we shall associate the e_g^π doublet with just a single orbital [136, 152], which, together with the other orbital mimicking the a_{1g} singlet, give rise to two bands, band 1 $\leftrightarrow a_{1g}$ and band 2 $\leftrightarrow e_g^\pi$, which accommodate one electron per site, i.e., they are quarter filled.

The other ingredient that is necessary to properly describe VO_2 is the electron-electron Coulomb interaction. However, since the main role that Coulomb repulsion is believed to play is to suppress charge fluctuations on V^{4+} , we shall ignore the long range tail and replace Coulomb repulsion with a short-range interaction.

Finally, we need to include the coupling to the lattice. For simplicity, we shall focus our attention only on the rutile and monoclinic M1 phases, as such ignoring the M2 phase, which is actually regarded by some as just a metastable modification of the M1 structure [40, 44, 146]. Under this assumption, we can model the lattice antiferrodistortion through a two-component zone boundary mode at momentum \mathbf{Q} , with displacement $\mathbf{X} = (X_1, X_2)$ and classical potential energy $\Phi(X_1, X_2)$. The X_1 and X_2 components model, respectively, the dimerising out-of-plane displacement and the band-splitting basal-plane one, see Fig. 1 [135, 153].

The model Hamiltonian is thus written as the sum of three terms:

$$\mathcal{H} = \mathcal{H}_{\text{el}} + \Phi(X_1, X_2) + \mathcal{H}_{\text{el}-\mathbf{X}}. \quad (1)$$

\mathcal{H}_{el} is the purely electronic component reading:

$$\mathcal{H}_{\text{el}} = \sum_{a=1}^2 \sum_{\mathbf{k}} (\epsilon_{a\mathbf{k}} - \mu) n_{a\mathbf{k}} + \frac{U}{2} \sum_i n_i (n_i - 1), \quad (2)$$

where $n_{a,\mathbf{k}}$ is the occupation number at momentum \mathbf{k} of the band $a = 1, 2$, n_i the electron number operator at site i , μ the chemical potential used to enforce the quarter filling condition and, finally, U is the on-site Hubbard repulsion.

With the aim to reduce the number of independent Hamiltonian parameters, we assume that the density-of-states (DOS) $\mathcal{D}_1(\epsilon)$ and $\mathcal{D}_2(\epsilon)$, of the band 1 and 2, respectively, have same bandwidth and centre of gravity, which we shall take as the zero of energy. In addition, we consider both DOS symmetric with respect to their centre, and such that $\epsilon_{1\mathbf{k}} = -\epsilon_{1\mathbf{k}+\mathbf{Q}}$, where \mathbf{Q} is the wave-vector of the antiferrodistortive mode \mathbf{X} . This assumption actually overestimates the dimerisation strength, since it entails that any $X_1 \neq 0$ is able to open a hybridisation gap in the middle of band 1, which, we remark, does not coincide with the chemical potential unless band 2 is pushed above it. This implies that a finite hybridisation gap within band 1 does not stabilise an insulator so long as band 2 still crosses the Fermi energy. Therefore our simplified modelling does not spoil the important feature that a distorted insulating phase

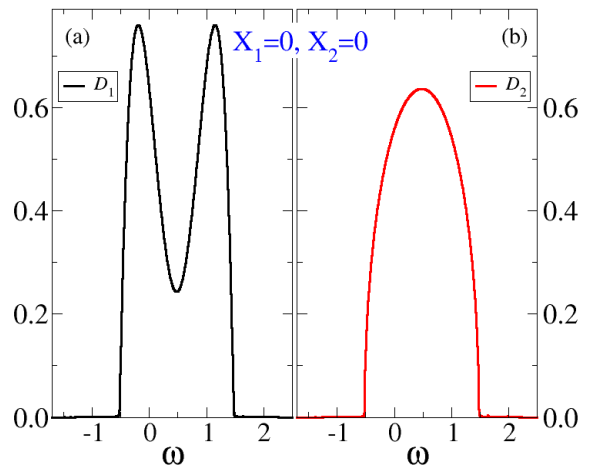


Figure 2. (Color online) The density-of-states $\mathcal{D}_a(\omega)$, $a = 1, 2$ for the two orbitals for $U = 0$, $X_1 = 0$ and $X_2 = 0$.

may occur only above a critical threshold of the Hamiltonian parameters, although it affects the value of that threshold, whose precise determination is however behind the scope of the present model-study.

In order to emphasise the bonding character of the a_{1g} , band 1, along the c_R axis, as opposed to the more isotropic e_g^π , band 2, we choose the following forms of the two corresponding DOS's:

$$\begin{aligned} \mathcal{D}_1(\epsilon) &= \frac{1}{\mathcal{N}} \left[a\epsilon^2 - b\epsilon^4 + D^2(bD^2 - a) \right], \\ \mathcal{D}_2(\epsilon) &= \frac{2}{\pi D} \sqrt{1 - \left(\frac{\epsilon}{D}\right)^2}, \end{aligned} \quad (3)$$

with $\epsilon \in [-D, D]$ and \mathcal{N} a normalisation factor. We take $b > a/D^2 > 0$ so that $\mathcal{D}_1(\epsilon)$ has a double-peak structure evocative of a one-dimensional DOS [71, 150, 154]. Hereafter, we take the half bandwidth $D = 1$ as our energy unit, and fix $aD^3 = 1.9$ and $bD^5 = 2.1$. The resulting DOS's are shown in Fig. 2 (a) and (b). There we note the two-peak structure of the band 1 DOS, mimicking the Van Hove singularities of a quasi one-dimensional band structure, in contrast to the structureless band 2 DOS.

We highlight that the electron-electron interaction in Eq. (2) only includes the monopole Slater integral $U > 0$, and not higher order multipoles responsible of Hund's rules. This approximation, that makes the analysis more transparent, requires some justification. The Coulomb interaction of a single Vanadium projected onto the t_{2g} manifold, which effectively behaves as an $l = 1$ atomic shell, can be written in terms of two Slater integrals as:

$$\begin{aligned} \mathcal{H}_{t_{2g}} &= \frac{U_{t_{2g}} - 3J_{t_{2g}}}{2} n^2 \\ &\quad - \frac{J_{t_{2g}}}{2} \left(4S(S+1) + L(L+1) \right), \end{aligned} \quad (4)$$

where n , S and L are the total occupation, spin, and angular momentum, respectively. Common values of the

parameters are $U_{t_{2g}} \simeq 4$ eV and $J_{t_{2g}} \simeq 0.68$ eV $\simeq U_{t_{2g}}/6$ [24]. Denoting as $E_0(n)$ the lowest energy with n electrons in the t_{2g} shell, the effective Hubbard U for V^{4+} can be defined through:

$$U = E_0(0) + E_0(2) - 2E_0(1) = U_{t_{2g}} - 3J_{t_{2g}} \simeq 1.96 \text{ eV}, \quad (5)$$

to be compared with the VO_2 bandwidth of about 2.6 eV [56]. In units of the half-bandwidth, $U \simeq 1.5$, the value we shall use hereafter [155, 156]. We observe that the Coulomb exchange $J_{t_{2g}}$ has no effect on the configurations with $n = 0, 1$, while it splits those with $n = 2$ in three multiplets, with $(S, L) = (0, 0), (1, 1), (0, 2)$, which are spread out over an energy $\simeq J_{t_{2g}}$, about a quarter of the full bandwidth. Such small value is not expected to qualitatively alter the physical behaviour, see, e.g., [157], which justifies our neglect of the exchange splitting in the model Hamiltonian (2).

We model the potential energy $\Phi(X_1, X_2)$ using a Landau functional for improper ferroelectrics [56, 75, 158] expanded up to the sixth order in the lattice displacements:

$$\Phi(X_1, X_2) = N \left[\frac{\alpha}{2} (X_1^2 + X_2^2) + \frac{\beta_1}{4} (2X_1 X_2)^2 + \frac{\beta_2}{4} (X_1^2 - X_2^2)^2 + \frac{\gamma}{6} (X_1^2 + X_2^2)^3 \right], \quad (6)$$

where N is the number of sites and the couplings α to γ are all positive. The terms proportional to α , i.e. the harmonic part of the potential, and that proportional to γ have full rotational symmetry in the X_1 - X_2 plane. On the contrary, β_1 favours a lattice distortion only along one of the two components, whereas β_2 a distortion with $|X_1| = |X_2|$. In the specific case of VO_2 , $\beta_2 > \beta_1$, and thus it is preferable to equally displace both modes [75] rather than just one of them.

Finally, we write the electron-lattice coupling as:

$$\begin{aligned} \mathcal{H}_{\text{el-X}} &= \mathcal{H}_{\text{el-X}}[X_1, X_2] \\ &= -\frac{g}{2} X_1 \sum_{\mathbf{k}\sigma} \left(c_{1\mathbf{k}\sigma}^\dagger c_{1\mathbf{k}+\mathbf{Q}\sigma} + \text{H.c.} \right) \\ &\quad - \frac{\delta}{2} X_2^2 \sum_{\mathbf{k}} \left(n_{1\mathbf{k}} - n_{2\mathbf{k}} \right), \end{aligned} \quad (7)$$

where $c_{1\mathbf{k}\sigma}$ creates an electron at momentum \mathbf{k} in orbital 1 with spin σ , and we recall that, by construction, $\epsilon_{1\mathbf{k}} = -\epsilon_{1\mathbf{k}+\mathbf{Q}}$. The dimerisation induced by the out-of-plane displacement X_1 is controlled by the coupling constant g , while δ parametrises the strength of the crystal field splitting generated by the basal-plane displacement X_2 . By symmetry, the coupling between the field X_1 and the electron dimerization is at leading order linear [135, 151]. The quadratic coupling in X_2 is intentional and has a physical explanation. Indeed, X_2 corresponds to the Vanadium displacement parallel to the diagonal of the rutile basal plane away from the centre of the Oxygen octahedron. As a result, the hybridisation between

the e_g^π and the Oxygen ligands closer to the new Vanadium position increases, whereas the hybridisation with the further Oxygens diminishes [150]. At linear order in the V-displacement X_2 , the two opposite variations of the hybridisation cancel each other, but, at second order, they add up to a net rise in energy of the e_g^π level, hence the expression in Eq. (7). The Hamiltonian Eq. (1) is invariant under the transformations $X_{1/2} \rightarrow -X_{1/2}$, reflecting a $Z_2 \times Z_2$ (also known as K_4 or ‘‘Viergruppe’’) symmetry.

Despite the great simplification effort, the model Hamiltonian Eq. (1) has still several parameters to be fixed. We emphasise that our main goal is to reproduce qualitatively the physics of VO_2 , without any ambition of getting also a quantitative agreement. Nonetheless, just to be sure not to explore a Hamiltonian parameter space completely detached from the real VO_2 compound, we choose parameters in line with the existing literature. We already mentioned our choice of $U = 1.5$, in units of the half-bandwidth, which is in line with the value used in realistic calculations [24, 48, 150, 159–161]. The other parameters involve the phonon variables. We shall choose $g = 0.4$, $\delta = 0.2$, $\alpha = 0.155$, $\beta_1 = 1.75 \cdot 10^{-3}$, $\beta_2 = 2\beta_1$ and $\gamma = 6.722 \cdot 10^{-4}$. Those values permit to reproduce the inter-band character of the band gap experimentally observed for the monoclinic insulator [87] and to obtain a size of it close enough to the experimental findings, see Sec. III A 1 for further details on the spectral properties of the system. Moreover, we checked *a posteriori* that we can reasonably reproduce the size of the electron-phonon interaction [136, 162, 163] and the lattice energy change across the rutile-to-monoclinic transition [163] as they were obtained in previous experiments or theoretical analysis. As a concluding remark, we point out that the direct experimental fits of the coupling constants is satisfactorily in agreement with previous estimations of the same [75, 164], further corroborating our choice of the parameter set.

III. DMFT SOLUTION

We solve the model Hamiltonian Eq. (1) by means of DMFT [165] within the adiabatic Born-Oppenheimer approximation. This approach will allow us to treat correlation effects non-perturbatively beyond an independent-particle description. Exploiting the Born-Oppenheimer approximation, we solve the electronic problem at a fixed displacement $\mathbf{X} = (X_1, X_2)$. To any choice of the displacement \mathbf{X} it corresponds to a different electronic problem through the electron-phonon coupling discussed above. Within DMFT such resulting interacting lattice electrons problem is mapped onto a quantum impurity model constrained by a self-consistency condition, which aim to determine the bath so to describe the local physics of the lattice model. The effective bath is described by a frequency dependent Weiss field $\mathcal{G}_{0,a}(i\omega_n)$, with $a = 1, 2$ the orbital index. The self-consistency condition relates

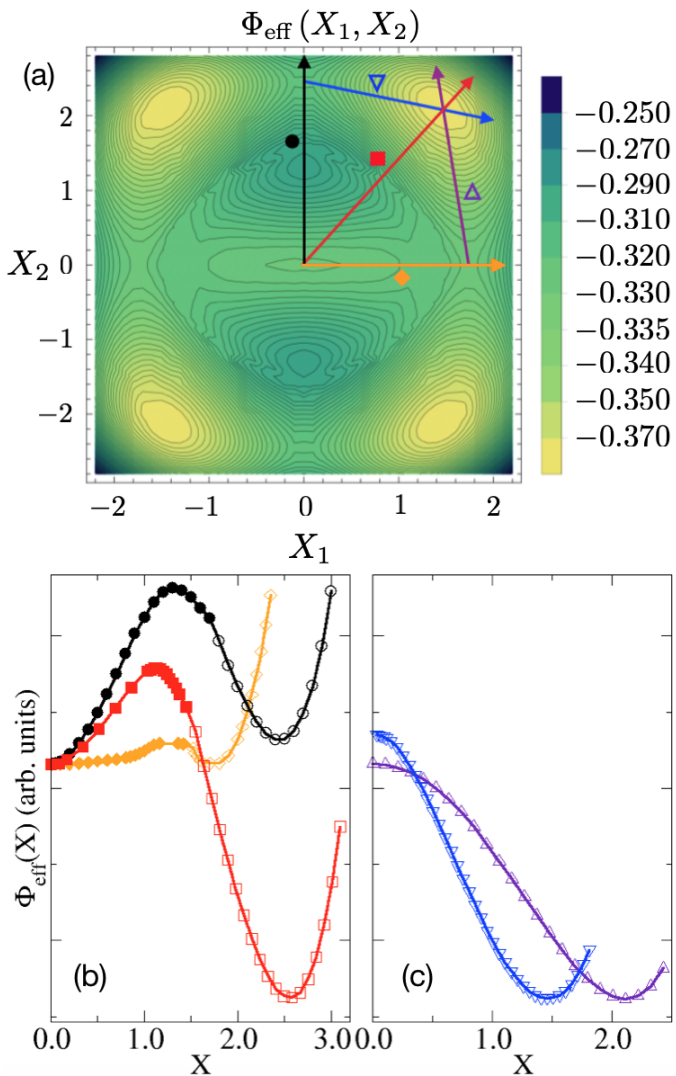


Figure 3. (Color online) (a) The zero-temperature colour map of the internal energy of the system as function of the amplitude of the crystal distortions X_1 and X_2 for $U = 1.5$. The system displays five minima, one at $X_1 = X_2 = 0$ corresponding to a metallic undistorted phase, the others at $X_1 \simeq \pm 1.5$ and $X_2 \simeq \pm 2.1$ corresponding to four equivalent insulating and distorted states. (b),(c) Evolution of the zero temperature internal energy along the paths shown in panel (a), where the symbols close to them correspond to the ones used in panels (b) or (c); the coordinate $X = \sqrt{X_1^2 + X_2^2}$ is computed along the lines as depicted in panel (a). Filled symbols correspond to a two band metallic solution, instead empty symbols correspond to an insulating solution everywhere except for the black curve with the circles, where they correspond to a single band metallic phase. Particularly, in panel (b): the circles (diamonds) correspond to the evolution of the internal energy along the line that involves just the distortion X_2 (X_1) and the squares correspond to the line that connects the undistorted metal and the distorted insulator found in the $X_1, X_2 > 0$ sector. In panel (c) the up-triangles (down-triangles) correspond to the line that connects the minimum observed in panel (b) along the line with the circles (diamonds) that involves just the distortion X_1 (X_2) to the global insulating minimum at $(X_1, X_2) = (1.5, 2.1)$.

the Weiss fields to the local self-energy function $\Sigma_a(i\omega_n)$, obtained from the solution of the effective quantum impurity model, and the local interacting Green's function

$$G_{\text{loc},a}(i\omega_n) = \int_{\mathbb{R}} d\varepsilon \mathcal{D}_a(\varepsilon) \frac{1}{\zeta_a - \varepsilon},$$

where $\zeta_a = i\omega_n + \mu - \Sigma_a(i\omega_n)$. The self-consistency conditions read:

$$\mathcal{G}_{0,a}^{-1}(i\omega_n) = G_{\text{loc},a}^{-1}(i\omega_n) + \Sigma_a(i\omega_n).$$

Once a Weiss field $\mathcal{G}_{0,a}(i\omega_n)$ is given, the solution to the DMFT equations is obtained iteratively as follows. We solve the effective quantum impurity problem associated to the given Weiss field using Exact Diagonalization technique [166, 167]. To this end, we discretize the effective bath into a number N_b of electronic levels [166–168]. The resulting Hamiltonian is diagonalized using Lanczos method and the ground-state (at zero temperature) or low lying states in the spectrum (at finite temperature) are determined [168]. The impurity Green's functions $G_a(i\omega_n)$ are then obtained using the dynamical Lanczos technique [165, 168]. The self-energy is obtained by solving the Dyson equation for the impurity problem $\Sigma_a(i\omega_n) = \mathcal{G}_{0,a}^{-1}(i\omega_n) - G_a^{-1}(i\omega_n)$. The self-energy is used to evaluate the local interacting Green's function and, finally, to update the Weiss fields by means of the self-consistency condition. The procedure is iterated until the overall error on the determination of the Weiss field falls below a threshold, which in our calculations was set to 10^{-6} . In this work, we use $N_b = 8$ as the total number of bath sites, corresponding to a finite system of $N = 10$ electronic levels or $N_s = 20$ spins. Yet, we tested our results with respect to larger values of N_b without finding significant differences.

Using the DMFT method we computed the electronic properties for several values of the displacement $\mathbf{X} = (X_1, X_2)$. The part of Eq. (7) related to the tilting X_2 enters in the single-particle term of the impurity hamiltonian as the usual crystal field splitting, while the dimerization X_1 acts directly on the density of states of band 1, see the expression of $\mathcal{D}_1(\varepsilon)$ appearing in Eq. (3), and it opens a gap of size $2gX_1$ in correspondence to its center of gravity.

We calculate the total electronic energy, or the free-energy at finite temperature, which renormalizes the Born-Oppenheimer adiabatic potential of the displacement $\Phi(X_1, X_2) \rightarrow \Phi_{\text{eff}}(X_1, X_2)$ through:

$$\Phi_{\text{eff}}(X_1, X_2) = \Phi(X_1, X_2) + \langle H_{\text{el}} \rangle + \langle H_{\text{el}-\mathbf{X}} \rangle. \quad (8)$$

We shall restrict our analysis to the paramagnetic sector forcing spin $SU(2)$ symmetry. However, we did check that magnetic solutions are higher in energy. We first present results at zero-temperature $T = 0$, and then move to those at $T > 0$.

A. Ground state phase diagram

In Fig. 3a we show the adiabatic potential $\Phi_{\text{eff}}(X_1, X_2)$ in (8) calculated by DMFT at $U = 1.5$. The energy landscape shows five minima. A local minima is located at the origin $X_1 = X_2 = 0$, and corresponds to an undistorted metal that we identify with the R phase of Vanadium dioxide. Four degenerate global minima are instead located at $X_1 \simeq \pm 1.5$ and $X_2 \simeq \pm 2.1$, which are related to each other by the $Z_2 \times Z_2$ symmetry and represent the four equivalent lattice distortions. We find that these global minima describe an insulating phase, and thus realize a two-band version of the Goodenough scenario [38] for the M1 phase, in qualitative agreement with *ab-initio* calculations of VO_2 [146, 147]. A detailed discussion of the electronic properties of all minima is postponed to the next Sec. III A 1.

In figures 3b and 3c we instead show the evolution of the adiabatic potential $\Phi_{\text{eff}}(X_1, X_2)$ along some specific lines, as indicated in Fig. 3a. We note that along the horizontal and vertical cuts, marked by a diamond and a circle in Fig. 3a, respectively, the energy landscape shows a saddle point, i.e., a minimum along the cut direction, but maximum in the perpendicular one. Within our model description, the effect of a uniaxial tensile strain would be taken into account by adding to the Hamiltonian Eq. (1) terms like: $-F_1 X_1^2$ or $-F_2 X_2^2$ ($F_1, F_2 > 0$), depending on the direction of the applied stress [169–171]. In presence of such terms, the saddle points observed in Fig. 3a along the lines $X_1 = 0$ or $X_2 = 0$ may turn into additional minima of the energy landscape [148], which can possibly describe the occurrence of the M2 phase in the framework of the same model Hamiltonian.

In order to understand what is the role of the Hubbard interaction U in stabilising the insulating solution, we studied the evolution of $\Phi_{\text{eff}}(X_1, X_2)$ for several values of U , along the line in the X_1 - X_2 plane connecting the rutile local minimum with one of the monoclinic global minima (the diagonal cut in Fig. 3a marked by a diamond symbol). Our results are reported in Fig. 4. We note that already at $U = 0$ the energy has two minima. One is at the origin and corresponds to the undistorted metal. The other is located at finite \mathbf{X} , and thus represents a distorted phase that must evidently be also insulating in order to be a local energy minimum. Therefore at small $U \lesssim 0.2$, the stable phase is the undistorted metal at $X = 0$ in Fig. 4, while the local minimum at $X \neq 0$ (monoclinic insulator) is metastable. However, for larger $U \gtrsim 0.2$, the situation is reversed: the distorted insulator becomes the global minimum, while the undistorted metal a local one, entailing the typical scenario of a first-order metal-insulator transition driven by interaction. The above results show that electron-electron interaction is crucial to stabilise the distorted insulator, though the active contribution of the lattice is equally essential. Indeed, the interaction strength, $U \simeq 1.5$ the half-bandwidth, is too small to drive on its own the metal-insulator transition [157]. In other words, the pic-

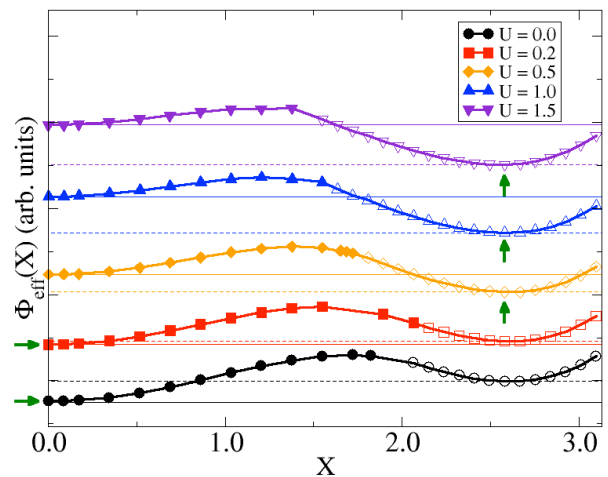


Figure 4. (Color online) The zero-temperature internal energy of the system (in arbitrary units) as function of the amplitude of the crystal distortion $X = \sqrt{X_1^2 + X_2^2}$ (coordinate taken along the line that connects the rutile solution and one of the monoclinic minima) for several values of the Hubbard interaction U . Filled (open) symbols correspond to a metallic (insulating) solution. The continuous (dashed) horizontal lines indicate the values of the metallic (insulating) minimum at each value of U . Arrows indicate the position of the absolute minimum for each value of the interaction.

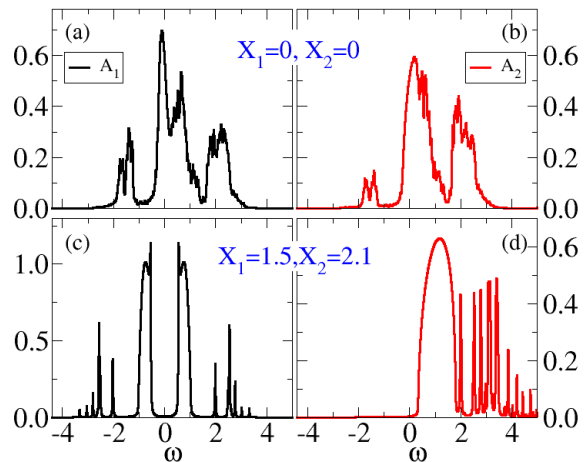


Figure 5. (Color online) The spectral functions $A_a(\omega)$, $a=1,2$ for the two minima shown in Fig. 4 at $U = 1.50$. The metallic phase correspond to $X = 0$ [(a) and (b)], instead the insulator corresponds to $X \sim 2.58$ [(c) and (d)].

ture that emerges from Fig. 4, with the interaction and the coupling to the lattice both necessary to stabilise the insulator, fully confirm our expectation in Sec. I.

1. Spectral functions

Further insights into the properties of the metal-insulator transition can be gained by looking at the spec-

tral functions:

$$A_a(\omega) = -\frac{1}{\pi} \text{Im} G_{loc,aa}(\omega) \quad (9)$$

where $a = 1, 2$ and $G_{loc,aa}$ is the local interacting Green's function obtained within the DMFT solution of the model. In Fig. 5 we show $A_a(\omega)$ at the different minima in 3a, with ω measured with respect to the chemical potential. We note that already in the absence of interaction, $U = 0$, the different shapes of the DOS's, see Fig. 2, lead to a larger occupation of band 1 than band 2. Such population unbalance is increased by $U > 0$, which effectively enhances the crystal field, leading to an even larger occupation of band 1 at expenses of 2 [152, 172, 173]. This is evident in the spectral function of the undistorted metal at $U = 1.5$, reported in Fig. 5(a) and Fig. 5(b), where the occupied $\omega \leq 0$ part of $A_1(\omega)$ overwhelms that of $A_2(\omega)$ more than in the $U = 0$ case of Fig. 2. We also note in the figures 5(a) and 5(b) side peaks that correspond to the precursors of the Hubbard bands.

The scenario is radically different in the insulating solution, see Fig. 5(c) and Fig. 5(d). Here we observe the formation of a hybridisation gap opening at the chemical potential inside the band 1. Two coherent-like features flank the gap. The band 2 is instead pushed above the Fermi energy, and therefore is empty. We still observe precursors of the Hubbard sidebands in $A_1(\omega)$, as well as signatures of the precursor of the upper Hubbard band in $A_2(\omega)$, though rather spiky because of the bath discretisation.

We note that in the insulating solution the lowest gap corresponds to transferring one electron from band 1 to band 2, i.e., from a_{1g} to e_g^π in the VO_2 language, and has a magnitude of about $E_{\text{gap}} \sim 0.8$ eV, for a realistic value of the half-bandwidth of 1.3 eV [56]. This value of the gap is not too far from the experimental one, $E_{\text{gap}}^{\text{ex}} \sim 0.6 - 0.7$ eV [35, 52, 119]. Therefore, our simplified modelling yields results that are not only qualitatively correct but, rather unexpectedly, also quantitatively not far off the actual ones. The band 1 \rightarrow band 2 transition, i.e., $a_{1g} \rightarrow a_{1g}$, though being slightly higher in energy, has a much steeper absorption edge since it involves the two coherent peaks in Fig. 5(c), already observed in previous works [24, 26, 27, 160]. This result is in loose agreement with XAS linear dichroism experiments [86, 174] that are able to distinguish the two absorption processes.

In order to assess the degree of electronic correlations, we calculate the quasiparticle residue of each band in the undistorted metal phase, defined by:

$$Z_a = \left(1 - \frac{\partial \text{Re} \Sigma_{aa}(\omega)}{\partial \omega} \right)_{|\omega=0}^{-1}, \quad (10)$$

with $a = 1, 2$. We find that the two bands at $X_1 = X_2 = 0$ show almost the same value $Z_{1/2} \sim 0.67$, not inconsistent with more realistic calculations [24, 72, 160, 175]. Such agreement, *a priori* not guaranteed, gives further support to our simple modelling.

IV. PHASE TRANSITION AT FINITE TEMPERATURE

Our main scope here is however to describe the first-order phase transition upon heating from the low-temperature M1 monoclinic insulator to the high-temperature rutile metal. In general, we can envisage a phase transition primarily driven either by the electron entropy or by the lattice one.

Indeed, we note that the electron free energy of the metal solution, which is metastable at $T = 0$, must drop faster upon raising temperature than the insulator free energy since the metal carries more electron entropy than the insulator. This effect alone, that is ignoring lattice entropy, would be able to drive a first-order transition when insulator and metal free energies cross. On the other hand, since the distorted ground state breaks the $Z_2 \times Z_2$ symmetry of the adiabatic lattice potential $\Phi_{\text{eff}}(X_1, X_2)$ in Fig. 3, we might expect such symmetry to be recovered by raising temperature only because of lattice entropy effects, i.e., ignoring the electronic contribution to entropy.

In reality, both effects should combine to drive the transition. However, dealing together with lattice and electron entropies within our computational scheme would imply to calculate the adiabatic potential $\Phi_{\text{eff}}(X_1, X_2)$ at any temperature, which is a rather heavy task. For this reason, in what follows we shall analyse separately electron and lattice entropy effects, and at the end argue what would happen should they act together.

A. Electron-driven transition

Let us first neglect the lattice entropy and study the temperature evolution of the free energies of the two inequivalent minima that we found at zero temperature. For that, we need to evaluate the electronic entropy, which can be obtained through:

$$\begin{aligned} S(X_1, X_2, T) &= \int_0^T dT' \frac{1}{T'} \frac{\partial \Phi_{\text{eff}}(X_1, X_2, T')}{\partial T'} \\ &= \int_{\Phi_{\text{eff}}(X_1, X_2, 0)}^{\Phi_{\text{eff}}(X_1, X_2, T)} \frac{d\Phi_{\text{eff}}}{T'(\Phi_{\text{eff}})}. \end{aligned} \quad (11)$$

The last equality corresponds to a change of integration variable from the temperature T' to the adiabatic potential Φ_{eff} , which is also the internal energy.

From the entropy S we can estimate the free energy:

$$F(X_1, X_2, T) = \Phi_{\text{eff}}(X_1, X_2, T) - TS(X_1, X_2, T), \quad (12)$$

which, we emphasise once more, does not include the lattice contribution to entropy. We shall compare the free energy of the undistorted metal solution at $\mathbf{X} = 0$, with that of the distorted insulator at $\mathbf{X} \neq 0$. In principle, the equilibrium displacement in the insulator should change

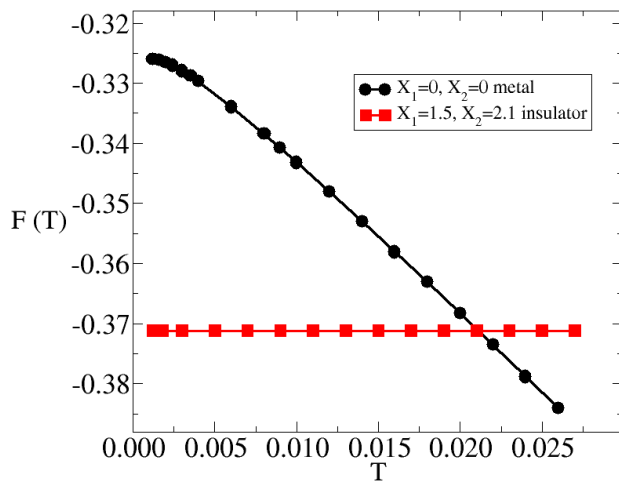


Figure 6. (Color online) Temperature evolution of the free energy at the two inequivalent minima $X_1 = X_2 = 0$ (dots) and $X_1 = 1.5, X_2 = 2.1$ (squares) observed at zero temperature for $U = 1.5$. The first-order transition occurs at $T_{\text{el}} \sim 0.021 \sim 320$ K, of the same order of magnitude as the experimental value 340 K.

with temperature. In practice, since the entropy of the insulator is negligible for all temperatures under consideration, we shall fix \mathbf{X} at the $T = 0$ value. The temperature evolution of the metal and insulator free energies so obtained are shown in Fig. 6. As expected, the larger entropy of the metal pushes its free energy below the insulator one at relatively low temperature, $T_{\text{el}} \sim 0.021$, substantially smaller than the insulating gap, and thus justifying our assumption of frozen \mathbf{X} . T_{el} identifies the insulator-metal transition, which is evidently first order since the two free energies cross with different slopes. Incidentally, $T_{\text{el}} \sim 0.021$ in half-bandwidth units, corresponds to ~ 320 K for a realistic bandwidth of 2.6 eV, which has the right order of magnitude when compared with the true critical temperature of 340 K. However, we should mention that a different choice of the parameters appearing in Eq. (1), keeping them still in a regime representative of the physics of Vanadium dioxide, would have produced a different value of T_{el} .

B. Lattice driven transition

We now move to study the properties of the lattice-driven transition. For that, we first need to model the lattice dynamics. However, since the tetragonal R to monoclinic M1 transition is a complex structural transformation, with martensitic features, especially in films [176–180], our modelling ought to be oversimplified, and aimed just to get qualitatively reasonable results, with no pretension of quantitative accuracy.

As a first step, we must relax our previous assumption of a global antiferrodistortive mode, and instead introduce a displacement field, i.e., a site dependent dis-

placement $\mathbf{X}_i = (X_{1i}, X_{2i})$. We assume that \mathbf{X}_i feels the local adiabatic potential $\Phi_{\text{eff}}(\mathbf{X}_i)$ of Fig. 3a, temperature independent since we are neglecting the electron entropy. In addition, we suppose that the displacements of nearest-neighbour sites are coupled to each other by an $SO(2) \cong U(1)$ invariant term that tends to minimise the strain. With those assumptions the classical Hamiltonian reads:

$$\mathcal{H}_{\text{ph}}(\mathbf{X}) = J \sum_{\langle ij \rangle} (\mathbf{X}_i - \mathbf{X}_j) \cdot (\mathbf{X}_i - \mathbf{X}_j) + \sum_i \Phi_{\text{eff}}(\mathbf{X}_i), \quad (13)$$

where \mathbf{X} denotes a configuration of all the displacement vectors. The model (13) is equivalent to a generalized XY-model, where \mathbf{X}_i plays the role of two-component spin of variable length, while $J > 0$ is the conventional spin stiffness. $\Phi_{\text{eff}}(\mathbf{X}_i)$ is the effective anisotropic potential obtained from the solution of the electron problem. Both the length and the direction of the local distortion \mathbf{X}_i are controlled by the effective potential $\Phi_{\text{eff}}(\mathbf{X}_i)$, which is not invariant under $U(1)$ but under separate $X_1 \rightarrow -X_1$ and $X_2 \rightarrow -X_2$ transformations, i.e., $Z_2 \times Z_2$. The phase diagram of an XY model in presence of an anisotropy term that lowers $U(1)$ down to Z_n is already known [181–183]. In particular, the anisotropy Z_n for $n \geq 4$ is a dangerously irrelevant perturbation that does not change the XY universality class of the transition [182, 183]. Our specific case study, where $U(1) \rightarrow Z_2 \times Z_2$, has not been considered yet, at least to our knowledge, but it should most likely change the XY universality class, which is what we are going to investigate in the following.

We study the classical model Eq. (13) at different temperatures using standard Monte Carlo (MC) method [184]. We consider the model on a three-dimensional cubic lattice of side N_x . The average value of a given observable, i.e. $\langle \mathcal{O} \rangle = \frac{1}{Z} \sum_{\mathbf{X}} \mathcal{O}(\mathbf{X}) e^{-\beta H_{\text{ph}}(\mathbf{X})}$, where $Z = \sum_{\mathbf{X}} e^{-\beta H_{\text{ph}}(\mathbf{X})}$, is therefore estimated statistically using MC algorithm to explore the configuration space. New configurations are generated and accepted/rejected using Metropolis algorithm with local updates. Each local update corresponds to a shift ΔX_i of one of the two component $i = 1, 2$, chosen with equal probability. Within our calculations we use $\Delta X_i = 0.15$, yet we checked that smaller values do not change the accuracy of the calculations. In addition, we include the possibility of global moves of the type $\mathbf{X}_i \rightarrow (-X_{1i}, X_{2i})$, $(X_{1i}, -X_{2i})$ or $(-X_{1i}, -X_{2i})$ with a total probability $P_{\text{global}} = 0.05$ equally distributed among the three cases, i.e. with probability $P_{\text{global}}/3$ each. The local updates require the evaluation of the effective potential $\Phi_{\text{eff}}(\mathbf{X}_i)$ at the new value of \mathbf{X}_i . To speed-up execution, we pre-evaluate all the interpolated values of the effective potential at any possible point compatible with the size of the shift using a bi-cubic spline method. A new configuration of the system is obtained after a full sweep of the

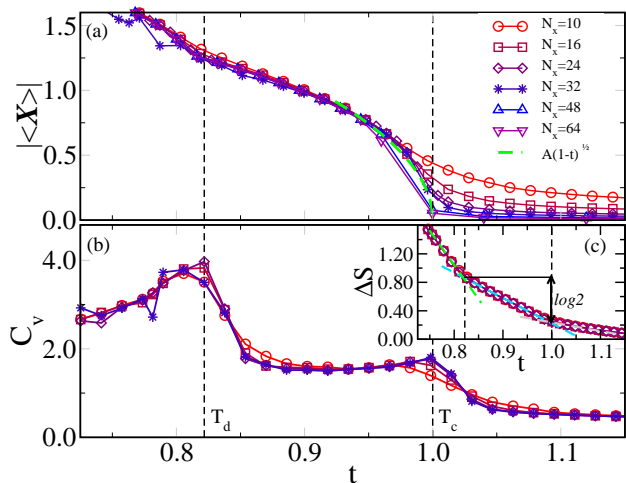


Figure 7. (Color online) (a) Modulus of the average displacement as function of the reduced temperature $t = T/T_c$. (b) Specific heat for the same model as in panel (a) as function of the reduced temperature. The data are for $N_s = 4 \times 10^5$ MC sweeps of the lattice and different linear size N_x (solid lines and open symbols). The dashed line in the critical region is a fit of the form $A(1-t)^{1/2}$, with $A = 0.96$. (c) Entropy loss $\Delta S = S_\infty - S(t)$ as a function of reduced temperature and N_x as in (a). S_∞ is the value attained in the limit of infinite temperature. The dashed lines are guides to the eye, emphasising the different linear behaviours of the entropy across the two phase transitions.

lattice sites. The statistical error is thus controlled by the number of sweeps N_s , to which it corresponds a number $N_s N_x^3$ of MC steps. In order to avoid self-correlation problems, we measure the average of any observables every $N_{\text{meas}} \simeq 100$ sweeps and in any case after a warm-up period of $N_{\text{wp}} \simeq 1000$ sweeps. In all our calculations, the number of sweeps is of the order of $N_s = 4 - 6 \times 10^5$. We further minimize the statistical error by executing the numerical computation in parallel with $N_{\text{cpu}} = 20$ cpu. The resulting statistical error is within the symbols in all our plots.

Before discussing the results, we have to mention that some details might depend on the precise form of the coupling between different sites. In the model Hamiltonian Eq. (13) we have chosen the simplest possible one, i.e. a nearest neighbor coupling, thus disregarding longer range interactions.

In Fig. 7(a) we plot the modulus of the average displacement, $|\langle \mathbf{X} \rangle|$, as function of the temperature. For small system size (e.g. $N_x = 10$) $|\langle \mathbf{X} \rangle|$ shows a smooth crossover in temperature. However, increasing N_x unveils the existence of a continuous phase-transition at a critical value T_c of the temperature. The actual value of T_c depends by the size of the coupling constant J , that somehow acts as a unit of measure for the energy. More involved calculations are necessary for the evaluation of J in Vanadium dioxide from first-principle calculations and we postpone them for a future work. For that reason, we

have preferred to use T_c as the unit of temperature in Fig. 7 and in those that follow. In order to better reveal the second order character of the transition, we also show in Fig. 7(a) the fit with a mean-field square-root behaviour. The fit is rather good, although we know that close to the transition the actual critical behaviour must deviate from mean-field.

A closer look to the temperature dependence of the order parameter uncovers a non-trivial two-step evolution, which is more evident in Fig. 7(b), where we show the specific heat $C_v = \partial \langle E \rangle / \partial T$ vs. T . Indeed, C_v clearly displays two peaks that are suggestive of two distinct transitions. The first transition at $T = T_c$, below which $|\langle \mathbf{X} \rangle|$ acquires a finite value, is followed by a second one at lower $T = T_d < T_c$.

From the knowledge of the specific heat at constant volume $C_v(T)$, we can compute the change of the vibrational entropy in the region where the two transitions occur as $\Delta S(t) = \int_t^\infty \frac{C_v(T)}{T} dT$. This quantity is displayed in Fig. 7(c) and it shows an almost linear behavior in the whole explored temperature range. However, as shown by the dashed lines there, the slopes of the line is different in the three regions $T < T_d$, $T_d < T < T_c$ and $T > T_c$.

In order to understand the nature of both transitions, in Fig. 8 we show at $T > T_c$, left panels, $T_d < T < T_c$, middle panels, and $T < T_d$, right panels, the endpoint distribution after $N_s = 4 \times 10^5$ MC sweeps of the lattice of the N_x^3 displacement vectors superimposed to the potential landscape in the (X_1, X_2) space (top panels), and a real space snapshot within a single layer of the cubic lattice (bottom panels). At high temperature, $T > T_c$, the \mathbf{X}_i 's cover homogeneously the whole potential landscape, see top-left panel, without any appreciable spatial correlation, see the bottom-left panel. Lowering T slightly below T_c , we observe a significant change in the displacement distribution, see middle panels. Specifically, the system seems to break ergodicity first along X_2 , in the simulation corresponding to the figure it localises in the $X_2 > 0$ half-plane, while it is still uniform along X_1 . Consequently, clusters of parallel displacement vectors form in real space. The alignment direction has $X_2 > 0$ for all clusters, while the X_1 component changes from cluster to cluster, see bottom-middle panel. Only below T_d , full ergodicity breakdown occurs, with the system trapped around just one of the four equivalent minima, in the figure that with $X_2 > 0$ and $X_1 > 0$. In other words, the $Z_2 \times Z_2$ symmetry of the model Eq. (13) gets broken in two steps upon cooling: first, the Z_2 symmetry $X_2 \rightarrow -X_2$ spontaneously breaks, and next, the residual $X_1 \rightarrow -X_1$ symmetry, leading to two consecutive Ising-like transitions. This is summarised in Fig. 9, where we see that at T_c $\langle X_2 \rangle$ becomes finite, and thus also $|\langle \mathbf{X} \rangle|$, while $\langle X_1 \rangle$ is still zero. Only below T_d also X_1 acquires a finite average value. Accordingly the vibrational entropy loss ΔS , shown in Fig. 7(c), changes of a quantity $\sim \ln(2)$ between the two temperatures T_d and T_c . This is consistent with an increase of the available phase space for the system of a factor of two by moving from one

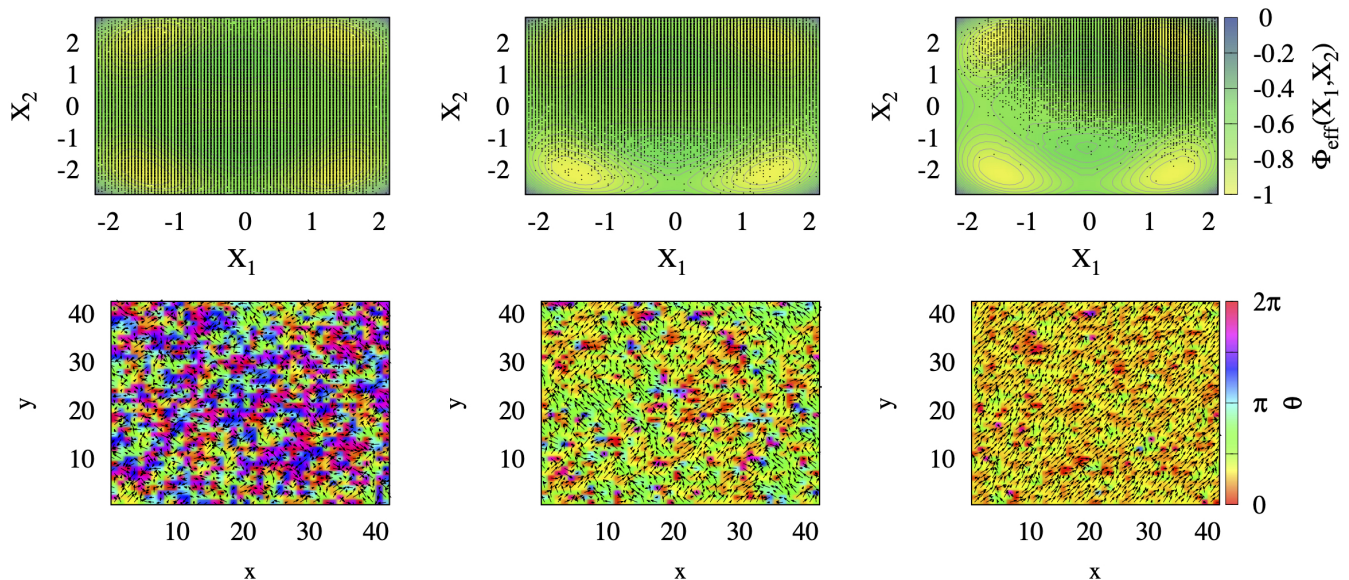


Figure 8. (Color online) *Top panels*: distribution of the displacements \mathbf{X}_i at the end of the MC simulation, superimposed to the adiabatic potential Φ_{eff} , properly normalised so that $\Phi_{\text{eff}} \in [-1, 0]$. Data are for $N_x = 50$, $N_s = 4 \times 10^5$ MC sweeps of the lattice, and reduced temperatures $t = T/T_c$: $t = 1.03$ (left), 0.82 (center), 0.71 (right). Each (black) dot represents one of the N_x^3 endpoints of the calculation. *Bottom panels*: displacement field configuration within a single plane of the cubic lattice, with the same parameters of the top panels. If $\mathbf{X}_i = |\mathbf{X}_i| (\cos \theta_i, \sin \theta_i)$, the color code represents $\theta_i \in [0, 2\pi]$, and the arrow length $|\mathbf{X}_i|$. At high temperature $T > T_c$ (left panels) \mathbf{X}_i have random length and orientation, thus covering homogeneously the entire potential landscape. For $T_d < T < T_c$ (center panels) the displacement orientation shows breaking of the Z_2 symmetry $X_2 \rightarrow -X_2$. At lower temperature $T < T_d < T_c$, also the residual Z_2 symmetry $X_1 \rightarrow -X_1$ gets broken; most of the \mathbf{X}_i 's have length and direction corresponding to just one of the potential global minima.

temperature to the other.

Translated in the language of VO_2 , these results suggest the existence of an intermediate monoclinic phase for $T_d < T < T_c$ where the V atoms are displaced only within the basal plane, i.e., the chains are tilted but not yet dimerised. In our model Hamiltonian (1), such phase with $\langle X_1 \rangle = 0$ describes a monoclinic metal, which, as discussed in Sec. I, has been reported in several experiments [81–83, 126–134]. Only below T_d , both components of the antiferrodistortive displacement are finite, leading to the M1 insulating phase.

In conclusion, without including the electron entropy we find two transitions that look continuous and in the Ising universality class: one at T_d between a monoclinic insulator and a monoclinic metal, and another at $T_c > T_d$ from the monoclinic metal to a rutile one. On the contrary, neglecting the lattice entropy and just including the electronic one, we found in Sec. IV A a single first-order transition at T_{el} , directly from the monoclinic insulator to the rutile metal. We can try now to argue what we could have obtained keeping both entropy contributions still within the Born-Oppenheimer adiabatic approximation.

In that case, we expect that the depth of the rutile minimum in the Born-Oppenheimer potential of Fig. 3 becomes a growing function of T , unlike the depth of

the insulating minima, since in the insulator the electronic entropy is negligible with respect to that in the metal. For the same reason, we expect that the height of the two equivalent saddle points at $X_1 = 0$ but $X_2 \simeq \pm 2.5$, see black and blue lines in panel (b) and panel (c), respectively, of Fig. 3, lowers with increasing T , since these points with large crystal field splitting but without dimerisation just describe the monoclinic metal, eventually turning these saddle points into local minima. This effect might well turn the monoclinic-insulator to monoclinic-metal transition at T_d into a first order one, all the more if we better modelled the martensitic features of the structural distortion. However, even in that case we still expect a further transition at $T_c > T_d$ into the rutile metal, unless the latter has such a large entropy compared to the monoclinic metal to drive a first order transition from the insulator directly into the rutile metal, as it would occur if $T_{\text{el}} < T_d$, i.e., if the electronic entropy gain far exceeds the lattice one.

The experimental evidences supporting the existence of a monoclinic metal phase intruding between the M1 insulator and R metal [81–83, 126–134] suggest that, should our modelling be indeed representative of VO_2 , then the Hamiltonian parameters should be such that $T_{\text{el}} \gtrsim T_d$. This also entails a substantial release of lattice entropy across the transition, in accordance with experiments [89, 185] and theoretical [186] proposals. We emphasise

that $T_{el} \gtrsim T_d$ does not mean that correlations play a minor role, but rather the opposite, since it would imply the insulator, whose internal energy is substantially contributed by electronic correlations, would survive up to much higher temperature if it were not for the lattice.

V. CONCLUSIONS

We have constructed a minimal model that we believe contains all essential ingredients to correctly capture the physics of the metal-insulator transition in vanadium dioxide.

The model comprises two orbitals per site, one mimicking the a_{1g} and the other the e_g^π , thus neglecting the twofold nature of the latter, which broaden into two bands. The a_{1g} band has a double peak structure reflecting its bonding character along the rutile c -axis, while the e_g^π one is structureless. Both have the same bandwidth and centre of gravity. The density corresponds to one electron per site, i.e., the two bands are at quarter filling. The electrons feel an on-site Hubbard repulsion, and are coupled to two zone-boundary lattice modes, corresponding, respectively, to the basal plane component, i.e., the tilting of the Vanadium chains, and out-of-plane component, responsible of the chain dimerisation, of the antiferrodistortive displacement that acquires a finite expectation value below the transition from the high temperature rutile structure to the low temperature monoclinic one (M1). Using realistic Hamiltonian parameters and assuming the Born-Oppenheimer adiabatic approximation, we find at low temperatures phase coexistence between a stable distorted insulator, the monoclinic M1 insulator, and a metastable undistorted metal, the rutile metal. Upon rising temperature, our model description suggests a two-step transition. First, the dimerisation component of the antiferrodistortive displacement melts, leading to a transition from the monoclinic insulator to a monoclinic metal. At higher temperature also the tilting component disappears, and the monoclinic metal turns into the rutile one. Such a two-transition scenario, not in disagreement with experiments, is mostly driven by the lattice entropy, also in accordance with experiments.

One of the messages of our model calculation is that the electron-electron interaction has the role to effectively enhance the coupling to the lattice, stabilising a distorted phase otherwise metastable in the absence of interaction. This also implies that we could have obtained similar results with weaker electronic correlations but stronger electron-lattice coupling. This conclusion is actually supported by the phenomenology of Niobium dioxide NbO_2 , which, *mutatis mutandis*, is akin to that of VO_2 . NbO_2 also undergoes a metal-insulator transition, though at substantially higher temperature of $T_{\text{MIT}} \sim 1080$ K [187–190]. There is some experimental evidence of separate structural and electronic phase transitions occurring in this compound [189–192], with a transition temperature for the structural change $T_s \sim 1123$ K [193], from a high-

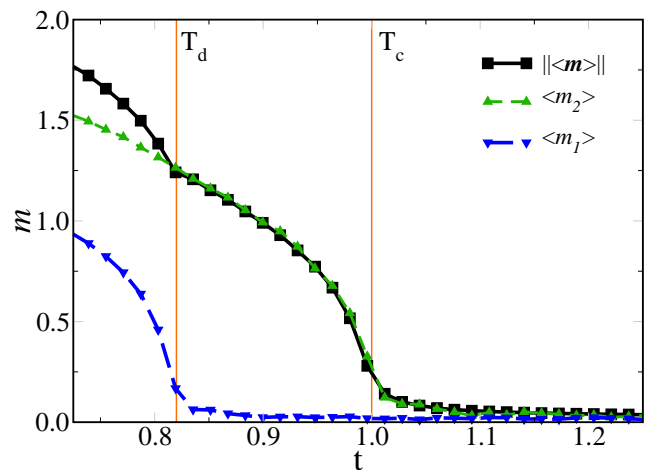


Figure 9. (Color online) magnetization m as a function of the reduced temperature $t = T/T_c$. Data are for $N_s = 6 \times 10^5$ MC sweeps, $N_x = 24$. The solid line (black with open square) is the modulus of the average magnetization vector. The dashed lines (green and blue with open triangles) indicate the behavior of the average of the magnetization components. The solid (orange) vertical lines indicate the two critical temperatures $T_d < T_c$ associated to the two stage transition.

temperature rutile structure to a low-temperature body centred tetragonal (BCT) one that locally resembles the M1 phase of VO_2 [191, 194–196]. It has been proposed that the mismatch between T_{MIT} and T_s can be justified by invoking a melting of the dimerization component of the structural distortion in the BCT insulator at smaller temperature as compared to the melting of the tilting component [190–192, 197]. The metallic solution that appears in between the two transition temperatures should be mostly metallic along the c_R axis, since the almost one dimensional a_{1g} band gives the most relevant contribution to the spectral weight at the Fermi level in this intermediate phase. This expectation is not in disagreement with some experimental findings in which they measure, above T_{MIT} , a metallic conductivity along c_R while a semiconducting one in the orthogonal direction [198]. However, we should point out that not all the experiments confirm this scenario [199]. We believe that a similar anisotropy in the conduction properties should be displayed also by the monoclinic metallic phase of Vanadium dioxide. The single $4d$ -electron in Nb^{4+} is expected to be less correlated than the $3d$ -electron in V^{4+} . This loss of correlations, testified by the VO_2 M2 phase having no counterpart in NbO_2 [200], and by the efficacy of *ab initio* methods to describe NbO_2 [74, 201–203], is actually overcompensated by the increase in covalency due to the broader spatial distribution of the $4d$ orbitals [204], which, in turn, yields a stronger coupling with the zone-boundary lattice modes, and thus a higher transition temperature.

ACKNOWLEDGEMENTS

F.G. likes to thank Sergiy Lysenko for the useful discussions about the thermodynamic potential for the two phononic modes, as well as for the choice of the parameters appearing there. F.G. thanks also Maja Berović and Daniele Guerci for the discussions concerning the manuscript. A.A. thanks Massimo Capone and Sandro

Sorella for useful discussions. We thank Martin Eckstein for fruitful debatings. We acknowledge support from the H2020 Framework Programme, under ERC Advanced Grant No. 692670 “FIRSTORM”. A.A. also acknowledges financial support from MIUR PRIN 2015 (Prot. 2015C5SEJJ001) and SISSA/CNR project “Superconductivity, Ferroelectricity and Magnetism in bad metals” (Prot. 232/2015).

-
- [1] Zheng Yang, Changhyun Ko, and Shriram Ramanathan, “Oxide electronics utilizing ultrafast metal-insulator transitions,” *Annual Review of Materials Research* **41**, 337–367 (2011).
- [2] T. Driscoll, Hyun-Tak Kim, Byung-Gyu Chae, Bong-Jun Kim, Yong-Wook Lee, N. Marie Jokerst, S. Palit, D. R. Smith, M. Di Ventra, and D. N. Basov, “Memory metamaterials,” *Science* **325**, 1518–1521 (2009).
- [3] J. Zhou, Y. Gao, Z. Zhang, H. Luo, C. Cao, Z. Chen, L. Dai, and X. Liu, “Vo₂ thermochromic smart window for energy savings and generation,” *Scientific Reports* **3**, 3029 (2013).
- [4] Wan-xia Huang, Xiao-gang Yin, Cheng-ping Huang, Qian-jin Wang, Teng-fei Miao, and Yong-yuan Zhu, “Optical switching of a metamaterial by temperature controlling,” *Applied Physics Letters* **96**, 261908 (2010).
- [5] Yujie Ke, Shancheng Wang, Guowei Liu, Ming Li, Timothy J. White, and Yi Long, “Vanadium dioxide: The multistimuli responsive material and its applications,” *Small* **14**, 1802025 (2018).
- [6] M. Liu, H. Y. Hwang, H. Tao, A. C. Strikwerda, K. Fan, G. R. Keiser, A. J. Sternbach, K. G. West, S. Kittiwatanakul, J. Lu, S. A. Wolf, F. G. Omenetto, X. Zhang, K. A. Nelson, and R. D. Averitt, “Terahertz-field-induced insulator-to-metal transition in vanadium dioxide metamaterial,” *Nature* **487**, 345 (2012).
- [7] N. I. Zheludev and Y. S. Kivshar, “From metamaterials to metadevices,” *Nature Materials* **11**, 917 (2012).
- [8] Mikhail A. Kats, Romain Blanchard, Shuyan Zhang, Patrice Genevet, Changhyun Ko, Shriram Ramanathan, and Federico Capasso, “Vanadium dioxide as a natural disordered metamaterial: Perfect thermal emission and large broadband negative differential thermal emittance,” *Phys. Rev. X* **3**, 041004 (2013).
- [9] Javier del Valle, Pavel Salev, Federico Tesler, Nicolás M. Vargas, Yoav Kalcheim, Paul Wang, Juan Trastoy, Min-Han Lee, George Kassabian, Juan Gabriel Ramírez, Marcelo J. Rozenberg, and Ivan K. Schuller, “Sub-threshold firing in mott nanodevices,” *Nature* , 1476–4687 (2019).
- [10] Caihong Zhang, Gaochao Zhou, Jingbo Wu, Yahua Tang, Qiye Wen, Shaoxian Li, Jianguang Han, Biaobing Jin, Jian Chen, and Peiheng Wu, “Active control of terahertz waves using vanadium-dioxide-embedded metamaterials,” *Phys. Rev. Applied* **11**, 054016 (2019).
- [11] Ernst Hoschek and Wilhelm Klemm, “Weitere beiträge zur kenntnis der vanadinoxide,” *Zeitschrift für anorganische und allgemeine Chemie* **242**, 63–69 (1939).
- [12] O. A. Cook, “High-temperature heat contents of v₂o₃, v₂o₄ and v₂o₅,” *Journal of the American Chemical Society* **69**, 331–333 (1947).
- [13] Georg Andersson, “Studies on vanadium oxides. i. phase analysis,” *Acta Chemica Scandinavica* **8**, 1599–1606 (1954).
- [14] M. S. Archer, D. S. P. Roebuck, and F. J. Whitby, “Magnetic susceptibility of vanadium dioxide,” *Nature* **174**, 754 (1954).
- [15] A. Magnéli and G. Andersson, “On the moo₂ structure type,” *Acta Chemica Scandinavica* **9**, 1378–1381 (1955).
- [16] Georg Andersson, “Studies on vanadium oxides. ii. the crystal structure of vanadium dioxide,” *Acta Chemica Scandinavica* **10**, 623–628 (1956).
- [17] W. Rüdorff, G. Walter, and J. Stadler, “Magnetismus, leitfähigkeit und reflexionsspektren von vanadindioxyd und vanadindioxyd-titandioxyd-mischkristallen,” *Zeitschrift für anorganische und allgemeine Chemie* **297**, 1–13 (1958).
- [18] F. J. Morin, “Oxides which show a metal-to-insulator transition at the neel temperature,” *Phys. Rev. Lett.* **3**, 34–36 (1959).
- [19] S. Westman, “Note on a phase transition in vo₂,” *Acta Chemica Scandinavica* **15**, 217 (1961).
- [20] W. Klemm and L. Grimm, “Über die wärmetönung bei der paramagnetischen curie-temperatur“ des vanadindioxyds,” *Naturwissenschaften* **27**, 787–787 (1939).
- [21] A. X. Gray, M. C. Hoffmann, J. Jeong, N. P. Aetukuri, D. Zhu, H. Y. Hwang, N. C. Brandt, H. Wen, A. J. Sternbach, S. Bonetti, A. H. Reid, R. Kukreja, C. Graves, T. Wang, P. Granitzka, Z. Chen, D. J. Higley, T. Chase, E. Jal, E. Abreu, M. K. Liu, T.-C. Weng, D. Sokaras, D. Nordlund, M. Chollet, R. Alonso-Mori, H. Lemke, J. M. Glowina, M. Trigo, Y. Zhu, H. Ohldag, J. W. Freeland, M. G. Samant, J. Berakdar, R. D. Averitt, K. A. Nelson, S. S. P. Parkin, and H. A. Dürr, “Ultrafast terahertz field control of electronic and structural interactions in vanadium dioxide,” *Phys. Rev. B* **98**, 045104 (2018).
- [22] Simon Wall, Shan Yang, Luciana Vidas, Matthieu Chollet, James M. Glowina, Michael Kozina, Tetsuo Katayama, Thomas Henighan, Mason Jiang, Timothy A. Miller, David A. Reis, Lynn A. Boatner, Olivier Delaire, and Mariano Trigo, “Ultrafast disordering of vanadium dimers in photoexcited vo₂,” *Science* **362**, 572–576 (2018).
- [23] Shi Chen, Zhaowu Wang, Hui Ren, Yuliang Chen, Wensheng Yan, Chengming Wang, Bowen Li, Jun Jiang, and Chongwen Zou, “Gate-controlled vo₂ phase transition for high-performance smart windows,” *Science Advances* **5** (2019), 10.1126/sciadv.aav6815.
- [24] S. Biermann, A. Poteryaev, A. I. Lichtenstein, and A. Georges, “Dynamical singlets and correlation-

- assisted peierls transition in VO_2 ,” *Phys. Rev. Lett.* **94**, 026404 (2005).
- [25] V. Eyert, “ VO_2 : A novel view from band theory,” *Phys. Rev. Lett.* **107**, 016401 (2011).
- [26] W. H. Brito, M. C. O. Aguiar, K. Haule, and G. Kotliar, “Metal-insulator transition in VO_2 : A DFT + DMFT perspective,” *Phys. Rev. Lett.* **117**, 056402 (2016).
- [27] O. Nájera, M. Civelli, V. Dobrosavljević, and M. J. Rozenberg, “Resolving the VO_2 controversy: Mott mechanism dominates the insulator-to-metal transition,” *Phys. Rev. B* **95**, 035113 (2017).
- [28] Dušan Plašienka, Roman Martoňák, and Marcus C. Newton, “Ab initio molecular dynamics study of the structural and electronic transition in VO_2 ,” *Phys. Rev. B* **96**, 054111 (2017).
- [29] O. Nájera, M. Civelli, V. Dobrosavljević, and M. J. Rozenberg, “Multiple crossovers and coherent states in a mott-peierls insulator,” *Phys. Rev. B* **97**, 045108 (2018).
- [30] Sooran Kim, Kyoo Kim, Chang-Jong Kang, and B. I. Min, “Correlation-assisted phonon softening and the orbital-selective peierls transition in VO_2 ,” *Phys. Rev. B* **87**, 195106 (2013).
- [31] J. H. Park, J. M. Coy, T. S. Kasirga, C. Huang, Z. Fei, S. Hunter, and D. H. Cobden, “Measurement of a solid-state triple point at the metal-insulator transition in VO_2 ,” *Nature* **500**, 431 (2013).
- [32] Y. Chen, S. Zhang, F. Ke, C. Ko, S. Lee, K. Liu, B. Chen, J. W. Ager, R. Jeanloz, V. Eyert, and J. Wu, “Pressure-temperature phase diagram of vanadium dioxide,” *Nano Letters* **17**, 2512–2516 (2017).
- [33] Weiss Alarich, “John b. goodenough: Magnetism and the chemical bond. interscience publishers. new york, london 1963. 393 seiten, 89 abbildungen. preis: Dm 95 s.” *Berichte der Bunsengesellschaft für physikalische Chemie* **68**, 996–996 (1964).
- [34] G. Villeneuve and P. Hagenmuller, “Metal-insulator transitions in pure and doped VO_2 ,” in *Localization and Metal-Insulator Transitions*, edited by H. Fritzsche and D. Adler (Springer US, Boston, MA, 1985) pp. 39–52.
- [35] C. N. Berglund and H. J. Guggenheim, “Electronic properties of VO_2 near the semiconductor-metal transition,” *Phys. Rev.* **185**, 1022–1033 (1969).
- [36] Y-R Jo, M-W Kim, and B-J Kim, “Direct correlation of structural and electrical properties of electron-doped individual VO_2 nanowires on devised tem grids,” *Nanotechnology* **27**, 435704 (2016).
- [37] Peter Baum, Ding-Shyue Yang, and Ahmed H. Zewail, “4d visualization of transitional structures in phase transformations by electron diffraction,” *Science* **318**, 788–792 (2007).
- [38] John B. Goodenough, “The two components of the crystallographic transition in VO_2 ,” *Journal of Solid State Chemistry* **3**, 490 – 500 (1971).
- [39] Augusto Marcelli, Marcello Coreno, Matus Stredansky, Wei Xu, Chongwen Zou, Lele Fan, Wangsheng Chu, Shiqiang Wei, Albano Cossaro, Alessandro Ricci, Antonio Bianconi, and Alessandro DElia, “Nanoscale phase separation and lattice complexity in VO_2 : The metal-insulator transition investigated by xanes via auger electron yield at the vanadium l23-edge and resonant photoemission,” *Condensed Matter* **2** (2017), 10.3390/condmat2040038.
- [40] J. P. Pouget, H. Launois, T. M. Rice, P. Dernier, A. Gosard, G. Villeneuve, and P. Hagenmuller, “Dimerization of a linear heisenberg chain in the insulating phases of $\text{V}_{1-x}\text{Cr}_x\text{O}_2$,” *Phys. Rev. B* **10**, 1801–1815 (1974).
- [41] A. Zylbersztejn and N. F. Mott, “Metal-insulator transition in vanadium dioxide,” *Phys. Rev. B* **11**, 4383–4395 (1975).
- [42] J. Pouget and H. Launois, “Metal-insulator phase transition in VO_2 ,” *Journal de Physique Colloques* **37**, C4–49–C4–57 (1976).
- [43] C. N. Berglund and A. Jayaraman, “Hydrostatic-pressure dependence of the electronic properties of VO_2 near the semiconductor-metal transition temperature,” *Phys. Rev.* **185**, 1034–1039 (1969).
- [44] J. P. Pouget, H. Launois, J. P. D’Haenens, P. Merenda, and T. M. Rice, “Electron localization induced by uniaxial stress in pure VO_2 ,” *Phys. Rev. Lett.* **35**, 873–875 (1975).
- [45] N. F. Quackenbush, H. Paik, M. J. Wahila, S. Sallis, M. E. Holtz, X. Huang, A. Ganose, B. J. Morgan, D. O. Scanlon, Y. Gu, F. Xue, L.-Q. Chen, G. E. Sterbinsky, C. Schlueter, T.-L. Lee, J. C. Woicik, J.-H. Guo, J. D. Brock, D. A. Muller, D. A. Arena, D. G. Schlom, and L. F. J. Piper, “Stability of the m2 phase of vanadium dioxide induced by coherent epitaxial strain,” *Phys. Rev. B* **94**, 085105 (2016).
- [46] M. Marezio, D. B. McWhan, J. P. Remeika, and P. D. Dernier, “Structural aspects of the metal-insulator transitions in cr-doped VO_2 ,” *Phys. Rev. B* **5**, 2541–2551 (1972).
- [47] T. M. Rice, H. Launois, and J. P. Pouget, “Comment on ” VO_2 : Peierls or mott-hubbard? a view from band theory”,” *Phys. Rev. Lett.* **73**, 3042–3042 (1994).
- [48] N. F. Mott and L. Friedman, “Metal-insulator transitions in VO_2 , Ti_2O_3 and $\text{Ti}_{2-x}\text{V}_x\text{O}_3$,” *The Philosophical Magazine: A Journal of Theoretical Experimental and Applied Physics* **30**, 389–402 (1974).
- [49] Alexander Pergament, “Metal-insulator transition: the mott criterion and coherence length,” *Journal of Physics: Condensed Matter* **15**, 3217 (2003).
- [50] Z. Zinamon and N. F. Mott, “Metal-non-metal transitions in narrow band materials; crystal structure versus correlation,” *The Philosophical Magazine: A Journal of Theoretical Experimental and Applied Physics* **21**, 881–895 (1970).
- [51] Philipp Werner, Emanuel Gull, Matthias Troyer, and Andrew J. Millis, “Spin freezing transition and non-fermi-liquid self-energy in a three-orbital model,” *Phys. Rev. Lett.* **101**, 166405 (2008).
- [52] M. M. Qazilbash, A. A. Schafgans, K. S. Burch, S. J. Yun, B. G. Chae, B. J. Kim, H. T. Kim, and D. N. Basov, “Electrodynamics of the vanadium oxides VO_2 and V_2O_3 ,” *Phys. Rev. B* **77**, 115121 (2008).
- [53] Sangwook Lee, Kedar Hippalgaonkar, Fan Yang, Jiawang Hong, Changyun Ko, Joonki Suh, Kai Liu, Kevin Wang, Jeffrey J. Urban, Xiang Zhang, Chris Dames, Sean A. Hartnoll, Olivier Delaire, and Junqiao Wu, “Anomalously low electronic thermal conductivity in metallic vanadium dioxide,” *Science* **355**, 371–374 (2017).
- [54] M. M. Qazilbash, M. Brehm, Byung-Gyu Chae, P.-C. Ho, G. O. Andreev, Bong-Jun Kim, Sun Jin Yun, A. V. Balatsky, M. B. Maple, F. Keilmann, Hyun-Tak Kim, and D. N. Basov, “Mott transition in VO_2 revealed by infrared spectroscopy and nano-imaging,” *Science* **318**, 1750–1753 (2007).

- [55] M. M. Qazilbash, K. S. Burch, D. Whisler, D. Shrekenhamer, B. G. Chae, H. T. Kim, and D. N. Basov, “Correlated metallic state of vanadium dioxide,” *Phys. Rev. B* **74**, 205118 (2006).
- [56] V. Eyert, “The metal-insulator transitions of VO_2 : A band theoretical approach,” *Annalen der Physik* **11**, 650–704 (2002).
- [57] A. Liebsch, H. Ishida, and G. Bihlmayer, “Coulomb correlations and orbital polarization in the metal-insulator transition of VO_2 ,” *Phys. Rev. B* **71**, 085109 (2005).
- [58] A. Continenza, S. Massidda, and M. Posternak, “Self-energy corrections in VO_2 within a model GW scheme,” *Phys. Rev. B* **60**, 15699–15704 (1999).
- [59] Matteo Gatti, Fabien Bruneval, Valerio Olevano, and Lucia Reining, “Understanding correlations in vanadium dioxide from first principles,” *Phys. Rev. Lett.* **99**, 266402 (2007).
- [60] R. Sakuma, T. Miyake, and F. Aryasetiawan, “Quasiparticle band structure of vanadium dioxide,” *Journal of Physics: Condensed Matter* **21**, 064226 (2009).
- [61] M. A. Korotin, N. A. Skorikov, and V. I. Anisimov, “Variation of orbital symmetry of the localized $3d^1$ electron of the V^{4+} ion upon the metal-insulator transition in VO_2 ,” *The Physics of Metals and Metallography* **94**, 17–23 (2002).
- [62] A. V. Kozhevnikov, V. I. Anisimov, and M. A. Korotin, “Calculation of the electronic structure of the vanadium dioxide VO_2 in the monoclinic low-temperature phase m_1 using the generalized transition state method,” *The Physics of Metals and Metallography* **104**, 215–220 (2007).
- [63] Xun Yuan, Yubo Zhang, Tesfaye A. Abteu, Peihong Zhang, and Wenqing Zhang, “ VO_2 : Orbital competition, magnetism, and phase stability,” *Phys. Rev. B* **86**, 235103 (2012).
- [64] R. Zhang, Q. S. Fu, C. Y. Yin, C. L. Li, X. H. Chen, G. Y. Qian, C. L. Lu, S. L. Yuan, X. J. Zhao, and H. Z. Tao, “Understanding of metal-insulator transition in VO_2 based on experimental and theoretical investigations of magnetic features,” *Scientific Reports* **8**, 17093 (2018).
- [65] Ricardo Grau-Crespo, Hao Wang, and Udo Schwingenschlögl, “Why the heyd-scuseria-ernzerhof hybrid functional description of VO_2 phases is not correct,” *Phys. Rev. B* **86**, 081101 (2012).
- [66] John E. Coulter, Efstratios Manousakis, and Adam Gali, “Limitations of the hybrid functional approach to electronic structure of transition metal oxides,” *Phys. Rev. B* **88**, 041107 (2013).
- [67] Zhiyong Zhu and Udo Schwingenschlögl, “Comprehensive picture of VO_2 from band theory,” *Phys. Rev. B* **86**, 075149 (2012).
- [68] Sheng Xu, Xiao Shen, Kent A. Hallman, Richard F. Haglund, and Sokrates T. Pantelides, “Unified band-theoretic description of structural, electronic, and magnetic properties of vanadium dioxide phases,” *Phys. Rev. B* **95**, 125105 (2017).
- [69] A. Moatti, R. Sachan, V. R. Cooper, and J. Narayan, “Electrical transition in isostructural VO_2 thin-film heterostructures,” *Scientific Reports* **9**, 3009 (2019).
- [70] G. Kotliar, SY Y Savrasov, K. Haule, V. S Oudovenko, O. Parcollet, and C. A Marianetti, “Electronic structure calculations with dynamical mean-field theory,” *Reviews of Modern Physics* **78**, 865–951 (2006).
- [71] A. S. Belozеров, M. A. Korotin, V. I. Anisimov, and A. I. Poteryaev, “Monoclinic M_1 phase of VO_2 : Mott-Hubbard versus band insulator,” *Phys. Rev. B* **85**, 045109 (2012).
- [72] Cédric Weber, David D. O’Regan, Nicholas D. M. Hine, Mike C. Payne, Gabriel Kotliar, and Peter B. Littlewood, “Vanadium dioxide: A peierls-mott insulator stable against disorder,” *Phys. Rev. Lett.* **108**, 256402 (2012).
- [73] M. S. Laad, L. Craco, and E. Müller-Hartmann, “Metal-insulator transition in rutile-based VO_2 ,” *Phys. Rev. B* **73**, 195120 (2006).
- [74] W. H. Brito, M. C. O. Aguiar, K. Haule, and G. Kotliar, “Dynamic electronic correlation effects in NbO_2 as compared to VO_2 ,” *Phys. Rev. B* **96**, 195102 (2017).
- [75] Nardeep Kumar, Armando Rúa, Félix E. Fernández, and Sergiy Lysenko, “Ultrafast diffraction conoscopy of the structural phase transition in VO_2 : Evidence of two lattice distortions,” *Phys. Rev. B* **95**, 235157 (2017).
- [76] Xun Yuan, Wenqing Zhang, and Peihong Zhang, “Hole-lattice coupling and photoinduced insulator-metal transition in VO_2 ,” *Phys. Rev. B* **88**, 035119 (2013).
- [77] Vance R. Morrison, Robert. P. Chatelain, Kunal L. Tiwari, Ali Hendaoui, Andrew Bruhács, Mohamed Chaker, and Bradley J. Siwick, “A photoinduced metal-like phase of monoclinic VO_2 revealed by ultrafast electron diffraction,” *Science* **346**, 445–448 (2014).
- [78] Martin R. Otto, Laurent P. René de Cotret, David A. Valverde-Chavez, Kunal L. Tiwari, Nicolas Émond, Mohamed Chaker, David G. Cooke, and Bradley J. Siwick, “How optical excitation controls the structure and properties of vanadium dioxide,” *Proceedings of the National Academy of Sciences* **116**, 450–455 (2019).
- [79] Zhensheng Tao, Tzong-Ru T. Han, Subhendra D. Mahanti, Phillip M. Duxbury, Fei Yuan, Chong-Yu Ruan, Kevin Wang, and Junqiao Wu, “Decoupling of structural and electronic phase transitions in VO_2 ,” *Phys. Rev. Lett.* **109**, 166406 (2012).
- [80] Serena A. Corr, Daniel P. Shoemaker, Brent C. Melot, and Ram Seshadri, “Real-space investigation of structural changes at the metal-insulator transition in VO_2 ,” *Phys. Rev. Lett.* **105**, 056404 (2010).
- [81] Jun-ichi Umeda, Sakichi Ashida, Hazime Kusumoto, and Koziro Narita, “A new phase appearing in metal-semiconductor transition in VO_2 ,” *Journal of the Physical Society of Japan* **21**, 1461–1462 (1966).
- [82] J. Laverock, S. Kittiwatanakul, A. A. Zakharov, Y. R. Niu, B. Chen, S. A. Wolf, J. W. Lu, and K. E. Smith, “Direct observation of decoupled structural and electronic transitions and an ambient pressure monoclinic-like metallic phase of VO_2 ,” *Phys. Rev. Lett.* **113**, 216402 (2014).
- [83] Tao Yao, Xiaodong Zhang, Zhihu Sun, Shoujie Liu, Yuanyuan Huang, Yi Xie, Changzheng Wu, Xun Yuan, Wenqing Zhang, Ziyu Wu, Guoqiang Pan, Fengchun Hu, Lihui Wu, Qinghua Liu, and Shiqiang Wei, “Understanding the nature of the kinetic process in a VO_2 metal-insulator transition,” *Phys. Rev. Lett.* **105**, 226405 (2010).
- [84] D. Lee, B. Chung, Y. Shi, G.-Y. Kim, N. Campbell, F. Xue, K. Song, S.-Y. Choi, J. P. Podkaminer, T. H. Kim, P. J. Ryan, J.-W. Kim, T. R. Paudel, J.-H. Kang, J. W. Spinuzzi, D. A. Tenne, E. Y. Tsymbal, M. S. Rz-

- chowski, L. Q. Chen, J. Lee, and C. B. Eom, “Isostructural metal-insulator transition in VO_2 ,” *Science* **362**, 1037–1040 (2018).
- [85] E. Arcangeletti, L. Baldassarre, D. Di Castro, S. Lupi, L. Malavasi, C. Marini, A. Perucchi, and P. Postorino, “Evidence of a pressure-induced metallization process in monoclinic VO_2 ,” *Phys. Rev. Lett.* **98**, 196406 (2007).
- [86] A. X. Gray, J. Jeong, N. P. Aetukuri, P. Granitzka, Z. Chen, R. Kukreja, D. Higley, T. Chase, A. H. Reid, H. Ohldag, M. A. Marcus, A. Scholl, A. T. Young, A. Doran, C. A. Jenkins, P. Shafer, E. Arenholz, M. G. Samant, S. S. P. Parkin, and H. A. Dürr, “Correlation-driven insulator-metal transition in near-ideal vanadium dioxide films,” *Phys. Rev. Lett.* **116**, 116403 (2016).
- [87] N. B. Aetukuri, A. X. Gray, M. Drouard, M. Cossale, L. Gao, A. H. Reid, R. Kukreja, H. Ohldag, C. A. Jenkins, E. Arenholz, K. P. Roche, H. A. Dürr, M. G. Samant, and S. S. P. Parkin, “Control of the metal-insulator transition in vanadium dioxide by modifying orbital occupancy,” *Nature Physics* **9**, 661 (2013).
- [88] T. J. Huffman, C. Hendriks, E. J. Walter, Joonseok Yoon, Honglyoul Ju, R. Smith, G. L. Carr, H. Krakauer, and M. M. Qazilbash, “Insulating phases of vanadium dioxide are mott-hubbard insulators,” *Phys. Rev. B* **95**, 075125 (2017).
- [89] J. D. Budai, J. Hong, M. E. Manley, E. D. Specht, C. W. Li, J. Z. Tischler, D. L. Abernathy, A. H. Said, B. M. Leu, L. A. Boatner, R. J. McQueeney, and O. Delaire, “Metallization of vanadium dioxide driven by large phonon entropy,” *Nature* **515**, 535 (2014).
- [90] W. Paul, “The present position of theory and experiment for VO_2 ,” *Materials Research Bulletin* **5**, 691 – 702 (1970).
- [91] P. Lederer, H. Launois, J.P. Pouget, A. Casalot, and G. Villeneuve, “Contribution to the study of the metal-insulator transition in the $\text{V}_{1-x}\text{Nb}_x\text{O}_2$ system-iii theoretical discussion,” *Journal of Physics and Chemistry of Solids* **33**, 1969 – 1978 (1972).
- [92] Matteo Gatti, Giancarlo Panaccione, and Lucia Reining, “Effects of low-energy excitations on spectral properties at higher binding energy: The metal-insulator transition of VO_2 ,” *Phys. Rev. Lett.* **114**, 116402 (2015).
- [93] I.-H. Hwang, Z. Jin, C.-I. Park, and S.-W. Han, “The influence of structural disorder and phonon on metal-to-insulator transition of VO_2 ,” *Scientific Reports* **7**, 14802 (2017).
- [94] D. B. McWhan, J. P. Remeika, J. P. Maita, H. Okinaka, K. Kosuge, and S. Kachi, “Heat capacity of vanadium oxides at low temperature,” *Phys. Rev. B* **7**, 326–332 (1973).
- [95] D. B. McWhan, M. Marezio, J. P. Remeika, and P. D. Dernier, “X-ray diffraction study of metallic VO_2 ,” *Phys. Rev. B* **10**, 490–495 (1974).
- [96] Ramakant Srivastava and L. L. Chase, “Raman spectrum of semiconducting and metallic VO_2 ,” *Phys. Rev. Lett.* **27**, 727–730 (1971).
- [97] C. Sommers, R. De Groot, D. Kaplan, and A. Zylbersztein, “Cluster calculations of the electronic d-states in VO_2 ,” *J. Physique Lett.* **36**, 157–160 (1975).
- [98] G. J. Hyland, “On the electronic phase transitions in the lower oxides of vanadium,” *Journal of Physics C: Solid State Physics* **1**, 189 (1968).
- [99] Michèle Gupta, A. J. Freeman, and D. E. Ellis, “Electronic structure and lattice instability of metallic VO_2 ,” *Phys. Rev. B* **16**, 3338–3351 (1977).
- [100] G. Stefanovich, A. Pergament, and D. Stefanovich, “Electrical switching and mott transition in VO_2 ,” *Journal of Physics: Condensed Matter* **12**, 8837 (2000).
- [101] D. Maurer, A. Leue, R. Heichele, and V. Müller, “Elastic behavior near the metal-insulator transition of VO_2 ,” *Phys. Rev. B* **60**, 13249–13252 (1999).
- [102] F. Pintchovski, W.S. Glaunsinger, and A. Navrotsky, “Experimental study of the electronic and lattice contributions to the VO_2 transition,” *Journal of Physics and Chemistry of Solids* **39**, 941 – 949 (1978).
- [103] S. Wall, D. Wegkamp, L. Foglia, K. Appavoo, J. Nag, R.F. Haglund Jr, J. Stahler, and M. Wolf, “Ultrafast changes in lattice symmetry probed by coherent phonons,” *Nature Communications* **3**, 721 (2012).
- [104] C. Kübler, H. Ehrke, R. Huber, R. Lopez, A. Halabica, R. F. Haglund, and A. Leitenstorfer, “Coherent structural dynamics and electronic correlations during an ultrafast insulator-to-metal phase transition in VO_2 ,” *Phys. Rev. Lett.* **99**, 116401 (2007).
- [105] Daniel Wegkamp and Julia Stähler, “Ultrafast dynamics during the photoinduced phase transition in VO_2 ,” *Progress in Surface Science* **90**, 464 – 502 (2015).
- [106] P. Schilbe and D. Maurer, “Lattice dynamics in VO_2 near the metal-insulator transition,” *Materials Science and Engineering: A* **370**, 449 – 452 (2004), 13th International Conference on Internal Friction and Ultrasonic Attenuation in Solids.
- [107] J. R. Brews, “Symmetry considerations and the vanadium dioxide phase transition,” *Phys. Rev. B* **1**, 2557–2568 (1970).
- [108] A. Cavalleri, Cs. Tóth, C. W. Siders, J. A. Squier, F. Ráksi, P. Forget, and J. C. Kieffer, “Femtosecond structural dynamics in VO_2 during an ultrafast solid-solid phase transition,” *Phys. Rev. Lett.* **87**, 237401 (2001).
- [109] Zhuoran He and Andrew J. Millis, “Photoinduced phase transitions in narrow-gap mott insulators: The case of VO_2 ,” *Phys. Rev. B* **93**, 115126 (2016).
- [110] Yasuhiro H. Matsuda, Daisuke Nakamura, Akihiko Ikeda, Shojiro Takeyama, Yuji Muraoka, and Yuki Suga, “Magnetic-field-induced insulator-metal transition in W-doped VO_2 at 500 T,” arXiv e-prints, arXiv:2001.08580 (2020), arXiv:2001.08580 [cond-mat.str-el].
- [111] H. S. Choe, J. Suh, C. Ko, K. Dong, S. Lee, J. Park, Y. Lee, K. Wang, and J. Wu, “Enhancing modulation of thermal conduction in vanadium dioxide thin film by nanostructured nanogaps,” *Scientific Reports* **7**, 7131 (2017).
- [112] John B. Goodenough, “Direct cation-cation interactions in several oxides,” *Phys. Rev.* **117**, 1442–1451 (1960).
- [113] A. S. Barker, H. W. Verleur, and H. J. Guggenheim, “Infrared optical properties of vanadium dioxide above and below the transition temperature,” *Phys. Rev. Lett.* **17**, 1286–1289 (1966).
- [114] David Adler, “Insulating and metallic states in transition metal oxides,” (Academic Press, 1968) pp. 1 – 113.
- [115] Hiromu Sasaki and Akinori Watanabe, “A new growing method for VO_2 single crystals,” *Journal of the Physical Society of Japan* **19**, 1748–1748 (1964).
- [116] Larry A. Ladd and William Paul, “Optical and transport properties of high quality crystals of VO_2 near the

- metallic transition temperature,” *Solid State Communications* **7**, 425 – 428 (1969).
- [117] C. R. Everhart and J. B. MacChesney, “Anisotropy in the electrical resistivity of vanadium dioxide single crystals,” *Journal of Applied Physics* **39**, 2872–2874 (1968).
- [118] P.F. Bongers, “Anisotropy of the electrical conductivity of vo2 single crystals,” *Solid State Communications* **3**, 275 – 277 (1965).
- [119] Wei-Tao Liu, J. Cao, W. Fan, Zhao Hao, Michael C. Martin, Y. R. Shen, J. Wu, and F. Wang, “Intrinsic optical properties of vanadium dioxide near the insulator-metal transition,” *Nano Letters* **11**, 466–470 (2011), pMID: 21166443.
- [120] M. Nakano, K. Shibuya, D. Okuyama, T. Hatano, S. Ono, M. Kawasaki, Y. Iwasa, and Y. Tokura, “Collective bulk carrier delocalization driven by electrostatic surface charge accumulation,” *Nature* **487**, 459 (2012).
- [121] D. Okuyama, M. Nakano, S. Takeshita, H. Ohsumi, S. Tardif, K. Shibuya, T. Hatano, H. Yumoto, T. Koyama, H. Ohashi, M. Takata, M. Kawasaki, T. Arima, Y. Tokura, and Y. Iwasa, “Gate-tunable gigantic lattice deformation in vo2,” *Applied Physics Letters* **104**, 023507 (2014).
- [122] G. J. Hyland and A. W. B. Taylor, “Clausius-clapeyron equation and the v2o4, v2o3 phase transitions,” *Journal of the Physical Society of Japan* **21**, 819B–819B (1966).
- [123] Tatsuyuki Kawakubo and Takehiko Nakagawa, “Phase transition in vo2,” *Journal of the Physical Society of Japan* **19**, 517–519 (1964).
- [124] G.V. Chandrashekar, H.L.C. Barros, and J.M. Honig, “Heat capacity of vo2 single crystals,” *Materials Research Bulletin* **8**, 369 – 374 (1973).
- [125] Tomokuni Mitsuishi, “On the phase transformation of vo 2,” *Japanese Journal of Applied Physics* **6**, 1060 (1967).
- [126] Bong-Jun Kim, Yong Wook Lee, Sungyeoul Choi, Jung-Wook Lim, Sun Jin Yun, Hyun-Tak Kim, Tae-Ju Shin, and Hwa-Sick Yun, “Micrometer x-ray diffraction study of vo2 films: Separation between metal-insulator transition and structural phase transition,” *Phys. Rev. B* **77**, 235401 (2008).
- [127] Joyeeta Nag, Richard F. Haglund, E. Andrew Payzant, and Karren L. More, “Non-congruence of thermally driven structural and electronic transitions in vo2,” *Journal of Applied Physics* **112**, 103532 (2012).
- [128] Shixiong Zhang, Jung Yen Chou, and Lincoln J. Lauhon, “Direct correlation of structural domain formation with the metal insulator transition in a vo2 nanobeam,” *Nano Letters* **9**, 4527–4532 (2009), pMID: 19902918.
- [129] Hyun-Tak Kim, Yong Wook Lee, Bong-Jun Kim, Byung-Gyu Chae, Sun Jin Yun, Kwang-Yong Kang, Kang-Jeon Han, Ki-Ju Yee, and Yong-Sik Lim, “Monoclinic and correlated metal phase in vo2 as evidence of the mott transition: Coherent phonon analysis,” *Phys. Rev. Lett.* **97**, 266401 (2006).
- [130] T. L. Cocker, L. V. Titova, S. Fourmaux, G. Holloway, H.-C. Bandulet, D. Brassard, J.-C. Kieffer, M. A. El Khakani, and F. A. Hegmann, “Phase diagram of the ultrafast photoinduced insulator-metal transition in vanadium dioxide,” *Phys. Rev. B* **85**, 155120 (2012).
- [131] Suhas Kumar, John Paul Strachan, Matthew D. Pickett, Alexander Bratkovsky, Yoshio Nishi, and R. Stanley Williams, “Sequential electronic and structural transitions in vo2 observed using x-ray absorption spectroscopy,” *Advanced Materials* **26**, 7505–7509 (2014).
- [132] A. V. Ilinskiy, O. E. Kvashenkina, and E. B. Shadrin, “Nature of the electronic component of the thermal phase transition in vo2 films,” *Semiconductors* **46**, 1171–1185 (2012).
- [133] A. V. Ilinskiy, O. E. Kvashenkina, and E. B. Shadrin, “Phase transition and correlation effects in vanadium dioxide,” *Semiconductors* **46**, 422–429 (2012).
- [134] Changhong Chen, Renfan Wang, Lang Shang, and Chongfeng Guo, “Gate-field-induced phase transitions in vo2: Monoclinic metal phase separation and switchable infrared reflections,” *Applied Physics Letters* **93**, 171101 (2008).
- [135] D. C. Mattis and W. D. Langer, “Role of phonons and band structure in metal-insulator phase transition,” *Phys. Rev. Lett.* **25**, 376–380 (1970).
- [136] C J Hearn, “Phonon softening and the metal-insulator transition in vo 2,” *Journal of Physics C: Solid State Physics* **5**, 1317 (1972).
- [137] Jan M. Tomczak, Ferdi Aryasetiawan, and Silke Biermann, “Effective bandstructure in the insulating phase versus strong dynamical correlations in metallic vo2,” *Phys. Rev. B* **78**, 115103 (2008).
- [138] Tatsuyuki Kawakubo, “Crystal distortion and electric and magnetic transition in vo2,” *Journal of the Physical Society of Japan* **20**, 516–520 (1965).
- [139] C.J. Hearn, “The metal-insulator transition in vo2,” *Physics Letters A* **38**, 447 – 448 (1972).
- [140] G.J. Hyland, “Semiconductor \rightleftharpoons metal phase transitions,” *Journal of Solid State Chemistry* **2**, 318 – 331 (1970).
- [141] David Adler, Julius Feinleib, Harvey Brooks, and William Paul, “Semiconductor-to-metal transitions in transition-metal compounds,” *Phys. Rev.* **155**, 851–860 (1967).
- [142] T.K. Mitra, S. Chatterjee, and G.J. Hyland, “A l.c.o.a.o approach to the band structure of rutile vo2,” *Physics Letters A* **37**, 221 – 222 (1971).
- [143] S. Chattejee, T.K. Mitra, and G.J. Hyland, “A.p.w. band structure of metallic vo2,” *Physics Letters A* **42**, 56 – 58 (1972).
- [144] Ed Caruthers, Leonard Kleinman, and H. I. Zhang, “Energy bands of metallic vo2,” *Phys. Rev. B* **7**, 3753–3760 (1973).
- [145] Ed Caruthers and Leonard Kleinman, “Energy bands of semiconducting vo2,” *Phys. Rev. B* **7**, 3760–3766 (1973).
- [146] S. M. Woodley, “The mechanism of the displacive phase transition in vanadium dioxide,” *Chemical Physics Letters* **453**, 167 – 172 (2008).
- [147] Makondelele Netsianda, Phuti E. Ngoepe, C. Richard A. Catlow, and Scott M. Woodley, “The displacive phase transition of vanadium dioxide and the effect of doping with tungsten,” *Chemistry of Materials* **20**, 1764–1772 (2008).
- [148] A. Tselev, I. A. Luk’yanchuk, I. N. Ivanov, J. D. Budai, J. Z. Tischler, E. Strelcov, A. Kolmakov, and S. V. Kalinin, “Symmetry relationship and strain-induced transitions between insulating m1 and m2 and metallic r phases of vanadium dioxide,” *Nano Letters* **10**, 4409 (2010).
- [149] A. M. de Graaf and R. Luzzi, “Crystallographic distortion, electron-electron interaction and the metal-nonmetal transition,” *Helvetica Physica Acta* **41**, 764

- (1968).
- [150] D. Paquet and P. Leroux-Hugon, “Electron correlations and electron-lattice interactions in the metal-insulator, ferroelastic transition in VO_2 : A thermodynamical study,” *Phys. Rev. B* **22**, 5284–5301 (1980).
- [151] Jia Shi, Robijn Bruinsma, and Alan R Bishop, “Theory of vanadium dioxide,” *Synthetic Metals* **43**, 3527 – 3530 (1991), proceedings of the International Conference on Science and Technology of Synthetic Metals.
- [152] Matteo Sandri, Massimo Capone, and Michele Fabrizio, “Finite-temperature gutzwiller approximation and the phase diagram of a toy model for VO_3 ,” *Phys. Rev. B* **87**, 205108 (2013).
- [153] A O Sboychakov, A L Rakhmanov, and K I Kugel, “Effect of electron-lattice interaction on the phase separation in strongly correlated electron systems with two types of charge carriers,” *Journal of Physics: Condensed Matter* **22**, 415601 (2010).
- [154] M. W. Haverkort, Z. Hu, A. Tanaka, W. Reichelt, S. V. Streltsov, M. A. Korotin, V. I. Anisimov, H. H. Hsieh, H.-J. Lin, C. T. Chen, D. I. Khomskii, and L. H. Tjeng, “Orbital-assisted metal-insulator transition in VO_2 ,” *Phys. Rev. Lett.* **95**, 196404 (2005).
- [155] Bi-Ching Shih, Tesfaye A. Abteu, Xun Yuan, Wenqing Zhang, and Peihong Zhang, “Screened coulomb interactions of localized electrons in transition metals and transition-metal oxides,” *Phys. Rev. B* **86**, 165124 (2012).
- [156] A. Fujimori, I. Hase, H. Namatame, Y. Fujishima, Y. Tokura, H. Eisaki, S. Uchida, K. Takegahara, and F. M. F. de Groot, “Evolution of the spectral function in mott-hubbard systems with d^1 configuration,” *Phys. Rev. Lett.* **69**, 1796–1799 (1992).
- [157] Luca de’ Medici, Jernej Mravlje, and Antoine Georges, “Janus-faced influence of hund’s rule coupling in strongly correlated materials,” *Phys. Rev. Lett.* **107**, 256401 (2011).
- [158] A. P. Levanyuk and D. G. Sannikov, “Improper ferroelectrics,” *Soviet Physics Uspekhi* **17**, 199 (1974).
- [159] G. J. Hyland, “Lattice polarization and coulomb energies in VO_2 ,” *The Philosophical Magazine: A Journal of Theoretical Experimental and Applied Physics* **20**, 837–841 (1969).
- [160] Bence Lazarovits, Kyoo Kim, Kristjan Haule, and Gabriel Kotliar, “Effects of strain on the electronic structure of VO_2 ,” *Phys. Rev. B* **81**, 115117 (2010).
- [161] C. Sommers and S. Doniach, “First principles calculation of the intra-atomic correlation energy in VO_2 ,” *Solid State Communications* **28**, 133 – 135 (1978).
- [162] K. Okazaki, H. Wadati, A. Fujimori, M. Onoda, Y. Muraoka, and Z. Hiroi, “Photoemission study of the metal-insulator transition in $\text{VO}_2/\text{TiO}_2(001)$: evidence for strong electron-electron and electron-phonon interaction,” *Phys. Rev. B* **69**, 165104 (2004).
- [163] Michel van Veenendaal, “Ultrafast photoinduced insulator-to-metal transitions in vanadium dioxide,” *Phys. Rev. B* **87**, 235118 (2013).
- [164] Sergiy Lysenko, Nardeep Kumar, Armando Rúa, José Figueroa, Junqiang Lu, and Félix Fernández, “Ultrafast structural dynamics of VO_2 ,” *Phys. Rev. B* **96**, 075128 (2017).
- [165] Antoine Georges, Gabriel Kotliar, Werner Krauth, and Marcelo J. Rozenberg, “Dynamical mean-field theory of strongly correlated fermion systems and the limit of infinite dimensions,” *Rev. Mod. Phys.* **68**, 13–125 (1996).
- [166] Michel Caffarel and Werner Krauth, “Exact diagonalization approach to correlated fermions in infinite dimensions: Mott transition and superconductivity,” *Physical review letters* **72**, 1545–1548 (1994).
- [167] C. Weber, A. Amaricci, M. Capone, and P. B. PB Littlewood, “Augmented hybrid exact-diagonalization solver for dynamical mean field theory,” *Physical Review B* **86**, 1–5 (2012).
- [168] M Capone, L de’ Medici, and A Georges, “Solving the dynamical mean-field theory at very low temperatures using the Lanczos exact diagonalization,” *Phys. Rev. B* **76**, 245116 (2007).
- [169] Ia. A. Mogunov, F. Fernández, S. Lysenko, A.J. Kent, A.V. Scherbakov, A.M. Kalashnikova, and A.V. Akimov, “Ultrafast insulator-metal transition in VO_2 nanostructures assisted by picosecond strain pulses,” *Phys. Rev. Applied* **11**, 014054 (2019).
- [170] J. Cao, E. Ertekin, V. Srinivasan, W. Fan, S. Huang, H. Zheng, J. W. L. Yim, D. R. Khanal, D. F. Ogletree, J. C. Grossman, and J. Wu, “Strain engineering and one-dimensional organization of metal-insulator domains in single-crystal vanadium dioxide beams,” *Nature Nanotechnology* **4**, 732 (2009).
- [171] B.A. Strukov and A. P. Levanyuk, *Ferroelectric Phenomena In Crystals: Physical Foundations*. (Berlin ; Springer, 1998).
- [172] Matteo Sandri and Michele Fabrizio, “Nonequilibrium gap collapse near a first-order mott transition,” *Phys. Rev. B* **91**, 115102 (2015).
- [173] F. Grandi, A. Amaricci, M. Capone, and M. Fabrizio, “Correlation-driven lifshitz transition and orbital order in a two-band hubbard model,” *Phys. Rev. B* **98**, 045105 (2018).
- [174] T. C. Koethe, Z. Hu, M. W. Haverkort, C. Schüßler-Langeheine, F. Venturini, N. B. Brookes, O. Tjernberg, W. Reichelt, H. H. Hsieh, H.-J. Lin, C. T. Chen, and L. H. Tjeng, “Transfer of spectral weight and symmetry across the metal-insulator transition in VO_2 ,” *Phys. Rev. Lett.* **97**, 116402 (2006).
- [175] A. S. Belozero, A. I. Poteryaev, and V. I. Anisimov, “Evidence for strong coulomb correlations in the metallic phase of vanadium dioxide,” *JETP Letters* **93**, 70–74 (2011).
- [176] L. A. L. de Almeida, G. S. Deep, A. M. N. Lima, and H. Neff, “Thermal dynamics of VO_2 films within the metal-insulator transition: Evidence for chaos near percolation threshold,” *Applied Physics Letters* **77**, 4365–4367 (2000), <https://doi.org/10.1063/1.1334917>.
- [177] R. Lopez, T. E. Haynes, L. A. Boatner, L. C. Feldman, and R. F. Haglund, “Size effects in the structural phase transition of VO_2 nanoparticles,” *Phys. Rev. B* **65**, 224113 (2002).
- [178] Mei Pan, Jie Liu, Hongmei Zhong, Shaowei Wang, Zhi feng Li, Xiaoshuang Chen, and Wei Lu, “Raman study of the phase transition in VO_2 thin films,” *Journal of Crystal Growth* **268**, 178 – 183 (2004).
- [179] J. H. Claassen, J. W. Lu, K. G. West, and S. A. Wolf, “Relaxation dynamics of the metal-semiconductor transition in VO_2 thin films,” *Applied Physics Letters* **96**, 132102 (2010), <https://doi.org/10.1063/1.3370353>.
- [180] B. Viswanath and Shriram Ramanathan, “Direct in situ observation of structural transition driven actuation in VO_2 utilizing electron transparent cantilevers,”

- Nanoscale* **5**, 7484–7492 (2013).
- [181] T. Schneider and E. Stoll, “Molecular-dynamics study of a two-dimensional ferrodistorive XY model with quartic anisotropy,” *Phys. Rev. Lett.* **36**, 1501–1504 (1976).
- [182] Jorge V. José, Leo P. Kadanoff, Scott Kirkpatrick, and David R. Nelson, “Renormalization, vortices, and symmetry-breaking perturbations in the two-dimensional planar model,” *Phys. Rev. B* **16**, 1217–1241 (1977).
- [183] Jie Lou, Anders W. Sandvik, and Leon Balents, “Emergence of $u(1)$ symmetry in the 3d xy model with Z_q anisotropy,” *Phys. Rev. Lett.* **99**, 207203 (2007).
- [184] Kurt Binder and Dieter Heermann, *Monte Carlo Simulation in Statistical Physics*, 6th ed., Graduate Text in Physics (Springer International Publishing, 2019).
- [185] Lu Chen, Ziji Xiang, Colin Tinsman, Tomoya Asaba, Qing Huang, Haidong Zhou, and Lu Li, “Enhancement of thermal conductivity across the metal-insulator transition in vanadium dioxide,” *Applied Physics Letters* **113**, 061902 (2018).
- [186] Thomas A. Mellan, Hao Wang, Udo Schwingenschlögl, and Ricardo Grau-Crespo, “Origin of the transition entropy in vanadium dioxide,” *Phys. Rev. B* **99**, 064113 (2019).
- [187] R.F. Janninck and D.H. Whitmore, “Electrical conductivity and thermoelectric power of niobium dioxide,” *Journal of Physics and Chemistry of Solids* **27**, 1183 – 1187 (1966).
- [188] Melissa R. Beebe, J. Michael Klopff, Yuhan Wang, Salporn Kittiwatanakul, Jiwei Lu, Stuart A. Wolf, and R. Alejandra Lukaszew, “Time-resolved light-induced insulator-metal transition in niobium dioxide and vanadium dioxide thin films,” *Opt. Mater. Express* **7**, 213–223 (2017).
- [189] Katsuo Seta and Keiji Naito, “Calorimetric study of the phase transition in nbo_2 ,” *The Journal of Chemical Thermodynamics* **14**, 921 – 935 (1982).
- [190] C.N.R. Rao, G.Rama Rao, and G.V.Subba Rao, “Semiconductor-metal transitions in nbo_2 and $\text{nb}_{1-x}\text{v}_x\text{o}_2$,” *Journal of Solid State Chemistry* **6**, 340 – 343 (1973).
- [191] John B. Goodenough, “Metallic oxides,” *Progress in Solid State Chemistry* **5**, 145 – 399 (1971).
- [192] Pierre Tolédano and Jean-Claude Tolédano, “Order-parameter symmetries for the phase transitions of non-magnetic secondary and higher-order ferroics,” *Phys. Rev. B* **16**, 386–407 (1977).
- [193] T. Sakata, K. Sakata, and I. Nishida, “Study of phase transition in nbo_2 ,” *physica status solidi (b)* **20**, K155–K157 (1967).
- [194] Ajit R. Dhamdhere, Tobias Hadamek, Agham B. Posadas, Alexander A. Demkov, and David J. Smith, “Structural characterization of niobium oxide thin films grown on rtio_3 (111) and $(\text{la},\text{sr})(\text{al},\text{ta})\text{o}_3$ (111) substrates,” *Journal of Applied Physics* **120**, 245302 (2016).
- [195] Adrian A. Bolzan, Celesta Fong, Brendan J. Kennedy, and Christopher J. Howard, “A powder neutron diffraction study of semiconducting and metallic niobium dioxide,” *Journal of Solid State Chemistry* **113**, 9 – 14 (1994).
- [196] Zenji Hiroi, “Structural instability of the rutile compounds and its relevance to the metal-insulator transition of vo_2 ,” *Progress in Solid State Chemistry* **43**, 47 – 69 (2015).
- [197] Kimiko Sakata, “Note on the phase transition in nbo_2 ,” *Journal of the Physical Society of Japan* **26**, 582–582 (1969).
- [198] G. Bélanger, J. Destry, G. Perluzzo, and P. M. Raccach, “Electron transport in single crystals of niobium dioxide,” *Canadian Journal of Physics* **52**, 2272–2280 (1974).
- [199] Matthew J. Wahila, Galo Paez, Christopher N. Singh, Anna Regoutz, Shawn Sallis, Mateusz J. Zuba, Jatinkumar Rana, M. Brooks Tellekamp, Jos E. Boschker, Toni Markurt, Jack E. N. Swallow, Leanne A. H. Jones, Tim D. Veal, Wanli Yang, Tien-Lin Lee, Fanny Rodolakis, Jerzy T. Sadowski, David Prendergast, Wei-Cheng Lee, W. Alan Doolittle, and Louis F. J. Piper, “Evidence of a second-order peierls-driven metal-insulator transition in crystalline nbo_2 ,” *Phys. Rev. Materials* **3**, 074602 (2019).
- [200] J. Haines, J. M. Léger, A. S. Pereira, D. Häusermann, and M. Hanfland, “High-pressure structural phase transitions in semiconducting niobium dioxide,” *Phys. Rev. B* **59**, 13650–13656 (1999).
- [201] V Eyert, “The metal-insulator transition of NbO_2 : An embedded peierls instability,” *Europhysics Letters (EPL)* **58**, 851–856 (2002).
- [202] Andrew O’Hara, Timothy N. Nunley, Agham B. Posadas, Stefan Zollner, and Alexander A. Demkov, “Electronic and optical properties of nbo_2 ,” *Journal of Applied Physics* **116**, 213705 (2014).
- [203] Andrew O’Hara and Alexander A. Demkov, “Nature of the metal-insulator transition in NbO_2 ,” *Phys. Rev. B* **91**, 094305 (2015).
- [204] Franklin J. Wong, Nina Hong, and Shriram Ramanathan, “Orbital splitting and optical conductivity of the insulating state of nbo_2 ,” *Phys. Rev. B* **90**, 115135 (2014).